

Application of the Filtered-X LMS Algorithm for Disturbance Rejection in Time-Periodic Systems

by

Leslie Paige Fowler

Thesis submitted to the Faculty of the
Virginia Polytechnic Institute and State University
in partial fulfillment of the requirements for the degree of

Master of Science

in

Mechanical Engineering

APPROVED:

Harry H. Robertshaw, Chairman

William R. Saunders

Harley H. Cudney

May 3, 1996
Blacksburg, Virginia

Keywords: Adaptive Control, Filtered-X LMS, Time-Periodic, Disturbance Rejection, Helicopter Rotor Blade

APPLICATION OF THE FILTERED-X LMS ALGORITHM FOR DISTURBANCE REJECTION IN TIME-PERIODIC SYSTEMS

by

Leslie Paige Fowler

Harry H. Robertshaw, Chairman

Mechanical Engineering

Extensive disturbance rejection methods have been established for time-invariant systems. However, the development of these techniques has not focused on application to time-periodic systems in particular until recently. The filtered-X LMS algorithm is regarded as the best disturbance rejection technique for aperiodic systems by many, as has been proven in the acoustics industry for rejecting unwanted noise. Since this is essentially a feedforward approach, we might expect its performance to be good with respect to time-periodic systems in which the disturbance frequency is already known. The work presented in this thesis is an investigation of the performance of the filtered-X LMS algorithm for disturbance rejection in time-periodic systems. Two cases are examined: a generalized linear, time-periodic system and the helicopter rotor blade in forward flight.

Results for the generalized system show that the filtered-X LMS algorithm does converge for time-periodic disturbance inputs and can produce very small errors. For the helicopter rotor blade system the algorithm is shown to produce very small errors, with a 96%, or 14 dB, reduction in error from the open-loop system. The filtered-X LMS disturbance rejection technique is shown to provide a successful means of rejecting time-periodic disturbances for time-periodic systems.

Acknowledgments

I would like to thank those people who helped me through this project. I would like to first thank Dr. Harry Robertshaw for his encouragement, support and brainstorming sessions. Dan Cole gets a big thank-you; his guidance and advice were invaluable. Thanks to Dr. William Saunders for the brainstorming sessions and advice. I would also like to thank my other committee member, Dr. Harley Cudney for his help and support.

Lastly I would like to thank my fiancé, Christian Fowler, for his neverending support and understanding. Thanks for putting up with my busy schedule and stressful semester.

Contents

1	Introduction	1
2	Literature Review	4
2.1	Classical Control Techniques	4
2.1.1	Feedback Control	5
2.1.1.1	Pole Placement	5
2.1.1.2	PID Control	6
2.1.2	Feedforward Control	9
2.1.3	Hybrid Compensator Design	11
2.2	Modern Control Techniques	13
2.2.1	Linear Quadratic Regulator Control	14
2.3	Higher Harmonic Control	17
2.3.1	Detailed Description of Higher Harmonic Control	18
2.3.2	Individual Blade Control	21
2.4	Adaptive Control Techniques	22
2.5	Control Techniques Specific to Time-Periodic Systems	23
2.5.1	Output Feedback	23
2.5.2	Pole Placement	25
2.5.3	Adaptive Control Via the Pulse Response Method	26
2.5.4	Filtered-X LMS Algorithm	26
3	Time Periodic Systems	28
3.1	Solving Differential Equations with Time-Varying Coefficients	29
3.1.1	Discrete State-Space Solution to Differential Equations with Constant Coefficients	29

3.1.2	Discrete State-Space Solution to Differential Equations with Time-Varying Coefficients	31
3.2	Disturbance Models Using Augmented States	33
4	Adaptive Control	35
4.1	Adaptive Filtering	35
4.2	Least-Mean-Square Algorithm	39
4.3	Adaptive Inverse Control	40
4.4	Filtered-X LMS For Disturbance Rejection	42
4.5	Algorithm Considerations for Time-Varying Systems	45
5	Filtered-X LMS for Linear Time-Periodic Systems	46
5.1	Generalized Time-Varying System	46
5.1.1	Equation of Motion	46
5.1.2	Effect of the Convergence Parameter μ	50
5.1.3	Effect of the Number of Adaptive Weights	51
5.1.4	Effect of the Sampling Rate	55
5.1.5	Discussion of Generalized Time-Periodic System Results	57
5.2	Helicopter Rotor Blade System	57
5.2.1	Motivation for Application of Controller to Rotor Blade	57
5.2.2	Equation of Motion	59
5.2.3	Results	62
5.3	Controller Error	66
6	Conclusions	70
	References	72
	Vita	76

List of Figures

2.1	Block Diagram of Feedback Controller	5
2.2	Proportional Control Block Diagram	7
2.3	Block Diagram of Transfer Function for a PI Controller	8
2.4	Block Diagram of Transfer Function for a PID Controller	9
2.5	Block Diagram of Feedforward Controller	10
2.6	Block Diagram of Feedforward—Feedback Controller	11
2.7	Block Diagram of Feedforward — Feedback Compensator Method.....	12
2.8	Block Diagram of State-Space System	14
2.9	Block Diagram of Closed-Loop State-Space System with LSVF.....	14
2.10	Block Diagram Representation of Higher Harmonic Control	20
2.11	Individual Blade Control Via a Servoflap.....	21
4.1	Single-Input Adaptive Transversal Filter	35
4.2	Example of an Adaptive Linear Combiner	36
4.3	Inverse Plant Modeling	41
4.4	Adaptive Inverse Modeling of a Noisy Plant	42
4.5	Filtered-X LMS Algorithm.....	43
4.6	Filtered-X LMS Controller for Generalized Time-Periodic System.....	44
5.1	Error Time Response for Generalized System.....	48
5.2	Control Input Time Response for Generalized System.....	48
5.3	Weight Vector Time Responses for Generalized System	49
5.4	E versus μ , 8 Weights.....	50
5.5	E versus μ , 4 Weights.....	52

5.6 Comparison of Error Responses for Varying Number of Adaptive Weights and Identical Values for μ	53
5.7 Comparison of Error Responses for Varying Number of Adaptive Weights and Different Values for μ	54
5.8 Comparison of Error Time Responses for Different Values of T.....	56
5.9 Error Time Response for Helicopter Rotor Blade System.....	62
5.10 Close-Up of Error Time Response for Helicopter Rotor Blade System.....	63
5.11 Control Input Time Response for Helicopter Rotor Blade System.....	64
5.12 Weight Vector Time Responses for Helicopter Rotor Blade System.....	65
5.13 Close-up of Time Response of 7th Weight.....	65
5.14 Inverse Plant Modeling.....	67

List of Tables

5.1 Helicopter Rotor Blade Variables61

Chapter 1

Introduction

Nearly all dynamic systems possess undesirable characteristics such as unwanted noises and vibrations. Throughout the history of control theory, attempts have been made to alter systems in methodical manners, thereby setting precedents for other disturbance rejection applications. In fact, “the presence of disturbances is one of the main reasons for using control” [Åström, 1990]. Fundamental limitations are placed on a system when disturbances are imposed upon it [Åström, 1990]. Stability and robustness are affected by disturbances on a system. For example, the achievable bandwidth of a closed-loop system will be limited if there is measurement noise in a servo system [Åström, 1990]. A tracking system for a satellite might not perform as needed if unwanted disturbances are present in the system’s response. If these systems are to perform according to their design specifications, we must implement some sort of control on the system. There are several different ways in which control of a disturbance might be achieved. There are feedback, feedforward, and prediction methods — these may be implemented via classical control, modern control, or adaptive control techniques. A disturbance can be eliminated at the source, measured or estimated to elicit control.

These disturbances will affect both time-invariant and time-periodic systems. An example for a time-invariant system is eliminating a component of a system's response at a single frequency — this problem has been thoroughly investigated and many methods exist for viable solutions. However, these methods are for applications whose systems are aperiodic in nature (i.e. the differential equation describing the system has constant coefficients). Usually the application is for control over all times. However, several

systems in our world do not fit in this classification. In addition, in most instances the constant coefficient control methods do not generalize in a simple way to the case of time-periodic coefficients [Calico and Wiesel, 1984]. An example of a time-periodic system is a helicopter rotor blade which rotates around a shaft while also translating through space. This complicated behavior introduces complex disturbances on the blade which change as the blade rotates through 360° . The work presented here addresses the disturbance rejection problem for time-periodic systems.

Extensive disturbance rejection methods have been established for aperiodic systems. Current methods of rejection are passive techniques such as tuned absorbers and active techniques such as the Least-Mean-Square (LMS) method. However, until recently the development of these techniques has not focused on application to time-periodic systems in particular. A method called Higher Harmonic Control (HHC) was developed by the helicopter industry to reduce periodic vibrations in the rotor blades which are subsequently transferred to the fuselage. However, this technique has not been generalized to all periodic systems. The filtered-X LMS algorithm is regarded as the best disturbance rejection technique for aperiodic systems by many, as has been proven in the acoustics industry for rejecting unwanted noise. Thus we would like to know how this algorithm performs with regard to the control of time-periodic systems. The work presented in this thesis is an investigation of the performance of the filtered-X LMS algorithm to time-periodic systems. Two cases will be examined: a generalized time-periodic system and the helicopter rotor blade in forward flight.

The following chapter provides a review of disturbance rejection techniques, both active and passive. Chapter 3 derives the discretization of a continuous time-periodic system, since in industry this type of control would be implemented with digital hardware. Chapter 4 follows with a discussion of adaptive control and specifically the filtered-X LMS algorithm. Some considerations in implementing this algorithm for time-

periodic systems in particular are explained. Following this are the results of the control of two time-periodic systems using the filtered-X LMS algorithm. This chapter examines a general time-periodic system and the very specific case of a helicopter rotor blade. Chapter 6 provides interpretations and conclusions of the results along with recommendations for further work in the area of disturbance rejection for time-periodic systems.

Chapter 2

Literature Review

Many different techniques have been applied to the disturbance rejection problem in the past. For years, passive techniques were primarily used; however, with the advent of modern control theory, active control methods have become popular. And with the current advancements in the computing industry, adaptive methods are becoming increasingly popular means of active control. This chapter presents an overview of the major disturbance rejection techniques developed to date. This includes classical control, modern control, and adaptive control. In addition, research in the area of control of time-periodic systems in particular will be addressed. The reader will then have a foundation from which to see the extensions made here in regards to the need for further development of disturbance rejection techniques for time-periodic systems.

2.1 Classical Control Techniques

The most intuitive and oldest means of eliminating the effects of a disturbance is to attempt to attenuate the disturbance at the source. This often translates to corrective measures in the system. For example, modifying the electronics in a sensor so that the noise is reduced is one common application of this technique. Other examples are “reducing friction forces in a servo by using better bearings,” or moving “a sensor to a position where there are smaller disturbances” [Åström, 1990]. Although this method of reduction at the source is beautiful in its simplicity, it is often impossible to achieve.

2.1.1 Feedback Control

If the disturbances cannot be rejected at the source, feedback control can be used. For this method, the manner in which the disturbance enters the system must be known. It is necessary to be able to measure at least one variable that is affected by the disturbance. It is also necessary to have access to one control input variable that enters the system in the vicinity of the disturbance. In this way, the effects of the disturbance can be mitigated by using local feedback [Åström, 1990]. The remainder of this section explains two different feedback control methods.

2.1.1.1 Pole Placement

In classical feedback control, the poles and zeros of the system which produce desired specified roots are determined. A gain that results in a closed-loop system with these specified roots is then found. This is known as the pole placement or inverse root locus technique [Hale, 1988]. In this method, the system's sensitivity to disturbances is thus changed indirectly. However, as the poles are moved farther to the left of the imaginary axis in the s -plane, stability is improved but the system becomes more sensitive to disturbances. Figure 2.1 shows how this controller is implemented.

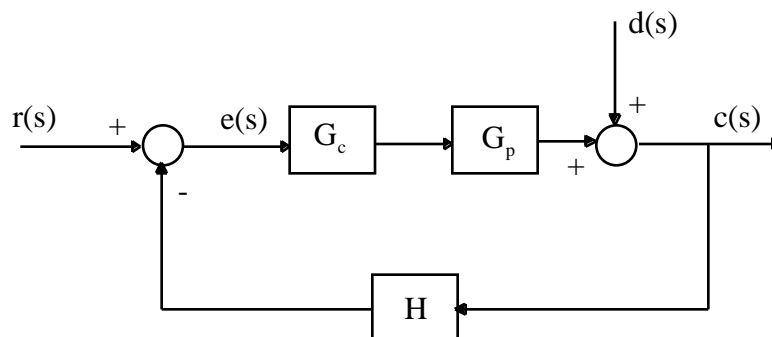


FIGURE 2.1 Block Diagram of Feedback Controller

Pole placement is limited in use, however, in that it must usually be able to withstand high gains in the control loop. This is because the algorithm does not have any upper limits on the control — the algorithm will simply choose the gains needed to place the poles where the designer specifies, no matter how large they may need to be. The farther the poles must be moved, the larger the feedback gains necessary. Thus “the dynamics relating the measured variable to the controlled variable should be such that a high-gain control can be used” [Åström, 1990]. The designer must always know the limitations of the control actuator to determine if the solution is feasible to implement. In addition to this limitation, the feedback transfer function H must be known or specified.

2.1.1.2 PID Control

PID, or proportional-integral-derivative, controllers were originally implemented with analog devices and have progressed through implementation schemes such as relays and motors, transistors, and finally integrated circuits. The controller consists of three parts, all of which work individually to alter the system dynamics in such a way as to produce the final desired results.

The proportional (P) controller is just simply a constant-gain feedback control. Often called a single-mode controller, this amplifier has a transfer function of the form

$$G_c = A \tag{2.1.1}$$

For a system transfer function G_p , the block diagram with this controller is shown in the following figure.

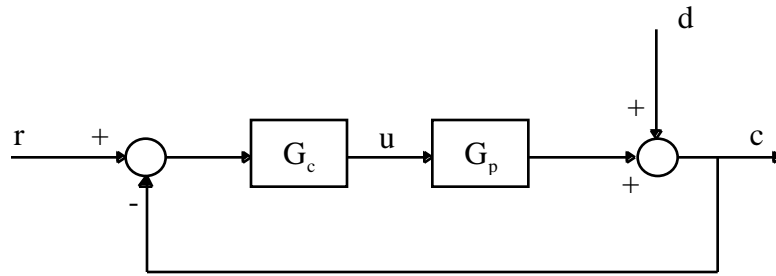


FIGURE 2.2 Proportional Control Block Diagram

Thus the control force entering the system is proportional to the error signal. For a proportional controller there is always a finite error, e , which decreases as the gain A is increased for type-0 systems; this error or offset can never be completely eliminated. As a result of this relationship, the gain A is often large in order for the controller to desensitize the system to step disturbances. In addition, a side effect of increasing the gain is a reduction in the damping ratio which could lead to undesirable effects.

In order to eliminate any step or bias error (or to follow a step input), an integrator is added to the system to create a two-mode (PI) controller with a transfer function of the form

$$\mathbf{G}_c = \frac{A \left(s + \frac{1}{\tau_I} \right)}{s} \quad (2.1.2)$$

where $1/\tau_I$ is the gain of the integrator. The corresponding block diagram for this transfer function is shown in Figure 2.3.

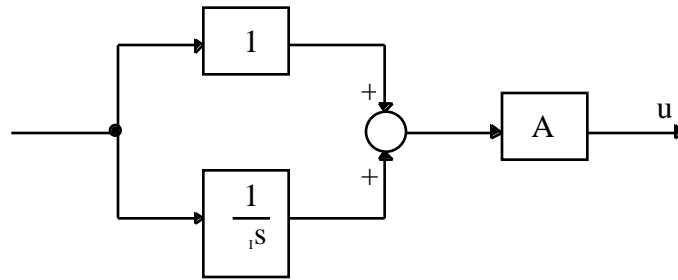


FIGURE 2.3 Block Diagram of Transfer Function for a PI Controller

The integrator directly changes the system's sensitivity to disturbances, specifically targeting step (bias) disturbances. As a result of this direct targeting, the gain A can be less than that of a proportional controller used alone.

The effect of the integrator is to add a pole at the origin thus making the error constant infinite and the error equal to zero. However, this added pole reduces the stability of the system and increases the number of oscillations in a step response in general. The peak overshoot is also increased in the step response. These effects can be minimized by increasing the value of τ_I , which moves the zero closer to the imaginary axis.

To reduce these negative effects of the integrator (number of oscillations, peak overshoot, and settling time), derivative control is added to create a three-mode (PID) controller. With this addition, the PID transfer function finally becomes

$$G_c = \frac{A \left(s + \frac{1}{\tau_I} + \tau_D s^2 \right)}{s} \quad (2.1.3)$$

and the resulting block diagram of this transfer function is shown in Figure 2.4.

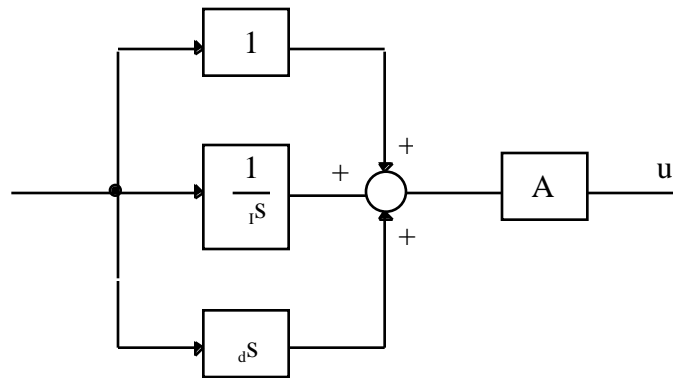


FIGURE 2.4 Block Diagram of Transfer Function for a PID Controller

Derivative control, which senses the rate of change of the actuating signal, decreases the settling time by speeding up the response and reduces the oscillatory behavior of the output. The process of selecting the controller parameters A , i , and d is performed using methods such as the Ziegler-Nichols settings, the reaction curve method, and the damped oscillation method [Hale, 1988].

This early compensation technique does not specifically reject the disturbance however; it acts to alter the resulting dynamics of the system when a disturbance is present. For this reason, it is really only useful for systems which have constant disturbances acting on them whose form is known.

2.1.2 Feedforward Control

If a disturbance can be measured or estimated, feedforward control is a useful method of canceling its effects on the system response. Unlike feedback control, this method is advantageous in that it is implemented by approximately compensating for disturbances

before they are sensed. In feedforward control, “a signal from a measurable disturbance is used to generate an appropriate control force to counteract or mitigate the effects of the disturbance” [Hale, 1988]. It minimizes the magnitude of the output for the disturbance input. Figure 2.5 shows how this technique is implemented.

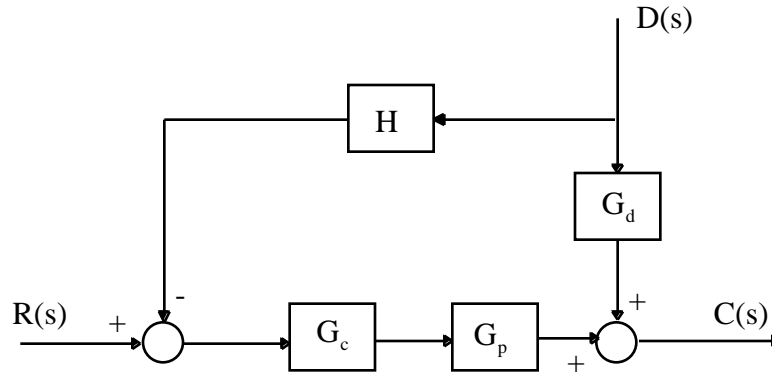


FIGURE 2.5 Block Diagram of Feedforward Controller

In this type of control the following relationship is desired:

$$\mathbf{D}\mathbf{G}_d - \mathbf{D}\mathbf{H}\mathbf{G}_c\mathbf{G}_p = \bar{\mathbf{0}} \quad (2.1.4)$$

This would require

$$\mathbf{H} = \frac{\mathbf{G}_d}{\mathbf{G}_c\mathbf{G}_p} \quad (2.1.5)$$

in order to isolate the system from any effects of \mathbf{D} [Fowler, *et al.*, 1995]. This is usually physically unrealizable. In practice, careful choice of \mathbf{G}_c , such as a simple gain, is usually sufficient to effectively minimize the effects of external disturbances [Hale, 1988].

2.1.3 Hybrid Compensator Design

Feedforward control can minimize transient errors but there are no guarantees of its accuracy due to its open-loop nature [Ogata, 1990]. Thus, the controller depicted in Figure 2.5 is unrealistic for most applications with unsuitable open-loop dynamics. For this reason, feedback control is often used coincidentally together with feedforward control to compensate for the latter's inaccuracies in minimizing the error. This is shown in Figure 2.6.

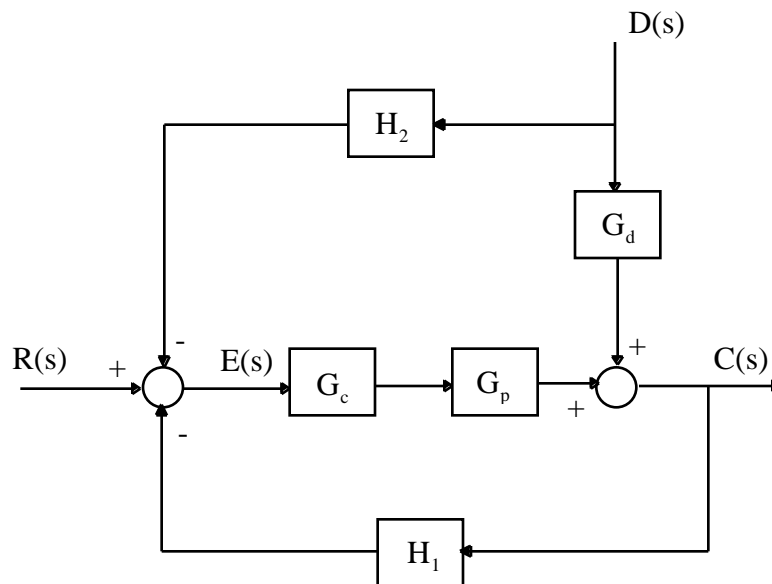


FIGURE 2.6 Block Diagram of Feedforward—Feedback Controller

Another variation on this is a compensator approach, derived by Ackermann [1985], shown in Figure 2.7.

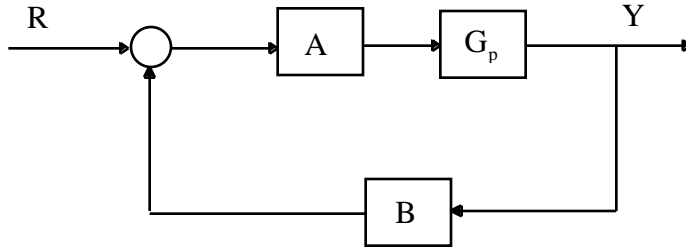


FIGURE 2.7 Block Diagram of Feedforward — Feedback Compensator Method

The control design works as follows. If you want to follow the input, as in tracking-type problems, the following equations hold in the discrete domain:

$$A(z) = R(z) \quad (2.1.6)$$

$$B(z) = 1 \quad (2.1.7)$$

If you do not want to follow the input, the transfer functions in the discrete domain are:

$$A = \# \text{ (arbitrary)} \quad (2.1.8)$$

$$B = R(z) \quad (2.1.9)$$

So, if the input is $R(t) = \sin at$ and you do not want to follow the input, using the relation

$$z = e^{jaT} \quad (2.1.10)$$

we find that the z-transform of $R(t)$ yields

$$B(z) = \frac{z \sin aT}{z^2 - 2 \cos aTz - 1} \quad (2.1.11)$$

This method is essentially a feedback technique with compensators placed in different places depending on the application. The disturbance (or an estimate of it) is fed forward. Compensators in the forward part of the loop or in the feedback part of the loop are used as appropriate to the application. This technique can then be used accordingly to reject unwanted disturbances by using equations 2.1.8 and 2.1.9 to not follow the input [Ackermann, 1985].

2.2 Modern Control Techniques

Classical control theories were developed primarily for single-input single-output (SISO) system design and analysis. After World War II, the emerging need for controlling systems with multiple inputs and outputs (MIMO) led to the development of what is now known as modern control. R. E. Kalman and others believed that state-space methods which were based on differential equation models were required to handle these more advanced systems. Numerous researchers agreed and as a result, the field of modern control evolved during the 1950's [Wolovich, 1994].

Neglecting disturbance inputs for the moment, the state-space representation of a system is defined by the following equations:

$$\dot{\mathbf{x}}(t) = \mathbf{A}\mathbf{x}(t) + \mathbf{B}\mathbf{u}(t) \quad (2.2.1)$$

$$\mathbf{y}(t) = \mathbf{C}\mathbf{x}(t) + \mathbf{D}\mathbf{u}(t) \quad (2.2.2)$$

where \mathbf{A} , \mathbf{B} , \mathbf{C} , and \mathbf{D} are determined from the differential equations describing a system. A block diagram depicting this system is shown in Figure 2.7.

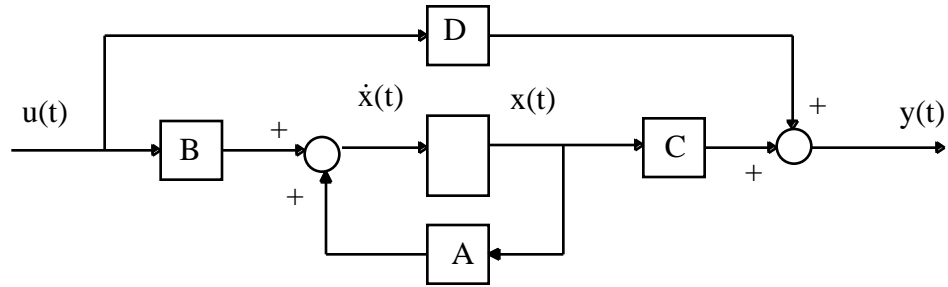


FIGURE 2.8 Block Diagram of State-Space System

2.2.1 Linear Quadratic Regulator Control

Kalman determined that a linear state variable feedback (LSVF) control law of the form

$$\mathbf{u}(t) = \mathbf{K}\mathbf{x}(t) + \mathbf{r}(t) \quad (2.2.3)$$

was optimal for minimizing a linear quadratic regulator (LQR) performance index. This control law results in the following block diagram:

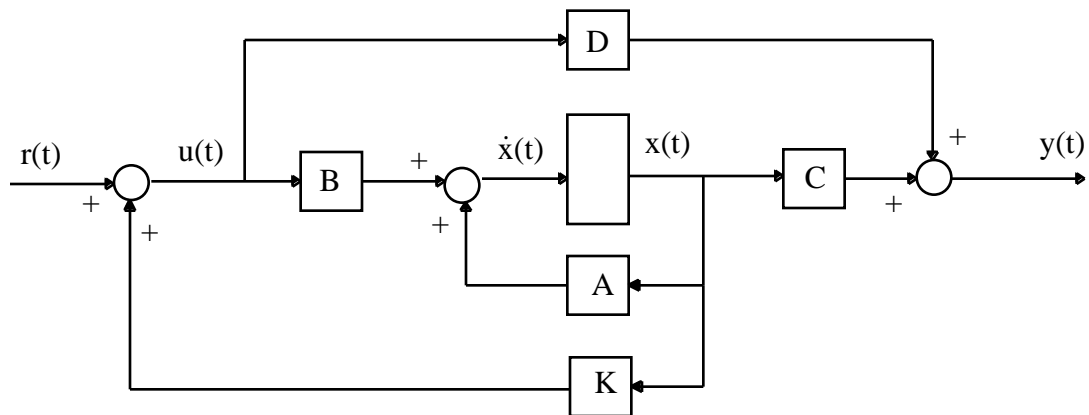


FIGURE 2.9 Block Diagram of Closed-Loop State-Space System with LSVF

Performance indexes are a way of obtaining desirable output regulation without requiring excessive input signals [Wolovich, 1994], as was evident with pole placement techniques for example. One of the most common and useful is the LQR performance index defined by equation (2.2.4):

$$J_{LQR} = \mathbf{x}^T \mathbf{M} \mathbf{x} + \int_0^{t_f} (\mathbf{x}^T \mathbf{Q} \mathbf{x} + \mathbf{u}^T \mathbf{R} \mathbf{u}) dt \quad (2.2.4)$$

where \mathbf{M} and \mathbf{Q} are symmetric positive semi-definite (PSD) matrices and \mathbf{R} is a real, symmetric positive definite (PD) matrix. \mathbf{M} is called the terminal penalty matrix, \mathbf{Q} is the state weighting matrix, and \mathbf{R} is the control weighting matrix.

Kalman determined that if a unique positive definite solution (steady-state) to the matrix Riccati equation,

$$\mathbf{Q} - \mathbf{P} \mathbf{B} \mathbf{R}^{-1} \mathbf{B}^T \mathbf{P} + \mathbf{P} \mathbf{A} + \mathbf{A}^T \mathbf{P} = 0 \quad (2.2.5)$$

is represented by \mathbf{P} , then the LSVF feedback law in equation (2.2.3) results in the minimization of J_{LQR} . The “minimization of J_{LQR} implies a desire to minimize both excessive output $y(t)$ excursions and the control $u(t)$ effort required to prevent such excursions” [Wolovich, 1994]. The adjustable weights \mathbf{M} , \mathbf{Q} , and \mathbf{R} can be used to obtain an appropriate compromise between these two conflicting goals [Wolovich, 1994]. The optimal control for this problem then becomes

$$\mathbf{u}^*(t) = -\mathbf{R}^{-1} \mathbf{B}^T \mathbf{P} \mathbf{x}(t) \quad (2.2.6)$$

Use of LQR control results in the optimal gain \mathbf{K} and optimal pole positions. This method works for time-invariant or time-varying systems and is just as easy for MIMO systems as for SISO systems. Like the classical control methods previously discussed however, this control method is a feedback approach which attempts to tailor the system response while not specifically rejecting a disturbance. However, we can adapt the state dynamics matrix so that a disturbance is rejected.

We must augment the system states to include the disturbance input so that the LQR controller can account for the effects of this unwanted input. This can be done when some assumptions about the form of the disturbance model can be made, as is the case for the work presented here. Specifically, the disturbances in this study are comprised of both a step input and periodic components — deterministic disturbances whose form can be modeled.

Given the differential equation of the system,

$$\dot{\mathbf{x}} = \mathbf{A}\mathbf{x} + \mathbf{B}\mathbf{u} + \mathbf{F}_d\mathbf{d} \quad (2.2.7)$$

we first define the state \mathbf{z} as follows:

$$\dot{\mathbf{z}} = \mathbf{A}_d\mathbf{z} \quad (2.2.8)$$

where

$$\mathbf{d} = \mathbf{C}_d\mathbf{z} \quad (2.2.9)$$

So given a known disturbance, \mathbf{d} , we can determine the matrices \mathbf{A}_d and \mathbf{C}_d . Augmenting the system states, \mathbf{x} , with the states \mathbf{z} yields the following:

$$\begin{pmatrix} \dot{\mathbf{x}}(t) \\ \dot{\mathbf{z}}(t) \end{pmatrix} = \begin{pmatrix} \mathbf{A}(t) & \mathbf{F}_d(t)\mathbf{C}_d \\ 0 & \mathbf{A}_d \end{pmatrix} \begin{pmatrix} \mathbf{x} \\ \mathbf{z} \end{pmatrix} + \begin{pmatrix} \mathbf{B}(t) \\ 0 \end{pmatrix} \mathbf{u}(t) \quad (2.2.10)$$

This is commonly written as

$$\dot{\boldsymbol{\xi}} = \mathbf{A}_a\boldsymbol{\xi} + \mathbf{B}_a\mathbf{u} \quad (2.2.11)$$

Now, the disturbance dynamics are included in the new state dynamics matrix, \mathbf{A}_a , (a state estimator is implemented to estimate these new states) and the LQR controller uses the estimated disturbance states in the state feedback implementation. The “construction of \mathbf{x} is improved by this disturbance observer and moreover a value \mathbf{z} is constructed which can be fed back to \mathbf{u} for compensation” [Ackermann, 1985]. Note that the augmentation of the states has no effect on the dynamics of the disturbance generator since it is uncontrollable from \mathbf{u} . With the formulation shown in equation 2.2.11 the effects of the disturbance \mathbf{d} can be reduced [Ackermann, 1985]. However, for time-periodic systems, this type of control may be ineffective due to the fact that the system dynamics are continually changing in time.

2.3 Higher Harmonic Control

One of the most common time-periodic systems is the helicopter rotor blade in forward flight. Due to the helicopter’s heavy use in military and commercial applications, controllers designed specifically for this system have been developed over the past few decades. Two basic approaches have been previously considered for the rotor blade control problem. In the first approach, commonly called higher harmonic control or HHC, an oscillatory modulation is superimposed on the basic pitch control of the swashplate. (The swashplate is comprised of two parallel plates, providing the means by which collective and cyclic pitch of the blades is achieved [Seddon, 1990].) Thus, all the blades are affected equally despite inherent differences in (the time dependent inputs to) each blade. The second approach, called individual blade control (IBC), denotes a method by which the pitch of each blade is controlled individually. These two approaches will now be discussed in more detail.

2.3.1 Detailed Description of Higher Harmonic Control

Higher harmonic control (HHC) is an active disturbance rejection technique which suppresses the vibrations due to periodic aerodynamic effects. These vibrations occur at known frequencies — at the rotor rotational frequency, ω , and at integer multiples thereof. The higher harmonic control technique is well suited to this problem of vibration isolation because it effectively places complex poles at the frequency of the disturbance in a feedback path, thus canceling the disturbance's effects. If the disturbance signal is available, the compensator can be implemented to provide a self-tuning, narrowband, vibration isolation method.

The HHC method was first developed by Shaw [1980, 1989] and has been expounded upon by numerous individuals [Hall, 1989, Johnson, 1982]. Several analytical investigations, flight tests, and wind-tunnel tests of HHC systems have demonstrated that these systems can produce substantial vibration reductions in forward flight [Robinson, 1991]. In HHC, rotor control inputs are applied at the harmonic frequencies where the vibrations are greatest. HHC superimposes an oscillatory modulation of frequency ω on the basic control pitch control of frequency ω [Ham, 1983, Reader and Dixon, 1984]. For a pitch motion described by

$$\theta(t) = \theta_0 - a_1 \cos \omega t - b_1 \sin \omega t \quad (2.3.1)$$

the general HHC input is expressed as

$$\begin{aligned} \theta(t) \sin \omega t &= (\theta_0 - a_1 \cos \omega t - b_1 \sin \omega t) \sin \omega t \\ &= \theta_0 \sin \omega t - \frac{a_1}{2} [\sin(\omega - \omega)t + \sin(\omega + \omega)t] - \frac{b_1}{2} [\cos(\omega - \omega)t + \cos(\omega + \omega)t] \end{aligned} \quad (2.3.2)$$

“HHC frequencies of the form $N\omega$ are usually used, thus resulting in pitch modulations not only at $N\omega$ but also at $(N-1)\omega$ and $(N+1)\omega$ ” [Giurgiutiu, *et al.*, 1994]. Usually, this

control is implemented via the swashplate by changing the pitch of the blade [Ham, 1983, Reader and Dixon, 1984].

The development of HHC as performed by Shaw is as follows. In his work the system dynamics are contained in a matrix \mathbf{T} , called the control response matrix, which is derived from $\mathbf{G}(j\omega_d)$ evaluated at the disturbance frequency ω_d . This matrix relates certain harmonics of the input to those same harmonics in the output. For a SISO system, this is expressed as

$$\mathbf{T} = \begin{bmatrix} a & b \\ -b & a \end{bmatrix} \quad (2.3.3)$$

where

$$\begin{aligned} a &= \text{Re}\{\mathbf{G}(j\omega_d)\} \\ b &= \text{Im}\{\mathbf{G}(j\omega_d)\} \end{aligned} \quad (2.3.4)$$

The sine and cosine components of the output at the disturbance frequency can be written as (for SISO systems)

$$\mathbf{z} = \mathbf{T}\mathbf{u} + \mathbf{z}_d \quad (2.3.5)$$

where \mathbf{z} is the vector of vibration amplitudes of the output, \mathbf{u} is the vector of input amplitudes, and \mathbf{z}_d is that part of the output which arises from the disturbance. Since \mathbf{z}_d is unknown, Shaw's approach is to multiply the output by \mathbf{T}^{-1} , which will provide the control needed to cancel \mathbf{z}_d . The resulting control input, for the continuous time case, is

$$\mathbf{u} = \mathbf{T}^{-1}\mathbf{z} \quad (2.3.6)$$

Figure 2.10 shows a block diagram representation of the HHC method. In the feedback loop, \mathbf{z} is multiplied by $\sin(\omega_d t)$ and $\cos(\omega_d t)$ and each branch is integrated to determine the sine and cosine components at the disturbance frequency. These signals are then multiplied by the inverse of the plant, \mathbf{T}^{-1} , and then modulated by $\sin(\omega_d t)$ and $\cos(\omega_d t)$. The signals are then added together again to form the control input to the system.

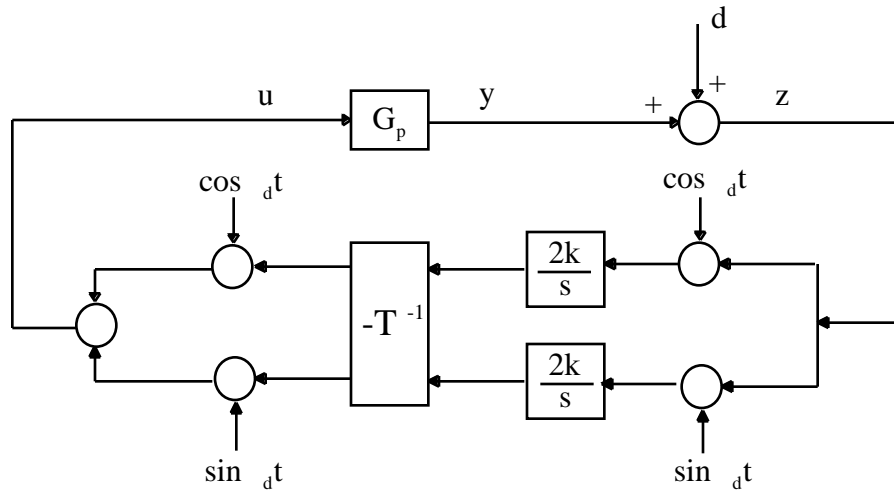


FIGURE 2.10 Block Diagram Representation of Higher Harmonic Control [Hall, 1989]

With HHC only one frequency is input to the system at a time. A more recent approach, called MHHC (multiple HHC), involves inputting several frequencies to the swashplate to reduce vibrations more effectively.

There are three drawbacks to the use of HHC: (1) the low-pass filter effects of the swashplate, (2) the controller is limited in its degrees of freedom, and (3) HHC affects all blades equally, regardless of manufacturing differences in the blades and differences in the dynamics of each blade as it rotates through 360° . The first issue is due to the fact that the swashplate is a low frequency device which as a result limits the frequency inputs of the controller [Giurgiutiu, *et al.*, 1994]. Thus the swashplate is very inefficient in regards to controlling a wide range of frequencies. This is an unavoidable characteristic of the control input mechanism. The second issue refers to the inherent limitations of swashplate control for rotors with four or more blades since there are only three degrees of freedom. To address the third issue, control has recently been achieved by individual blade pitch actuators [Ham, 1983, Reader and Dixon, 1984].

2.3.2 Individual Blade Control

In individual blade control (IBC), the rotor blades have their pitch motion controlled individually. This implementation of HHC thus addresses the problem discussed in issue (3) previously. In addition, the control is not restricted by the $N+1$, $N-1$ phenomenon characteristic of swashplate control. Finally, it has been found that IBC has improved frequency response as well [Giurgiutiu, *et al.*, 1994].

One possibility for implementation of individual blade control (IBC) consists in using an aerodynamic servoflap to provide the necessary control. Induced strain actuators mounted in the blade are connected to the servoflaps to provide the necessary motion (Figure 2.11) [Giurgiutiu, 1994].



FIGURE 2.11 Individual Blade Control Via a Servoflap

Other means of implementing IBC include replacing the conventional push-rods of the swashplate assembly with active devices such as hydraulic actuators [Jacklin, *et al.*, 1993].

In each of these methods of higher harmonic control, only feedback control techniques have been employed as a means of changing the system's response characteristics [Giurgiutiu, *et al.*, 1994, Millott and Friedmann, 1992, Nitzsche, 1992].

Thus the controller is not taking advantage of the fact that the disturbances are known for the helicopter rotor blade system.

2.4 Adaptive Control Techniques

Feedback control, specifically HHC, has been used extensively for vibration alleviation in the time-periodic rotor blade system. However, the use of feedforward control and adaptive feedforward methods such as filtered-X LMS have not been published for these applications to time-periodic systems. Widrow, *et al.* [1976] suggested that the inherently complex mathematics involved with nonstationary inputs and nonstationary adaptive filters is the primary cause of this.

Previously, disturbance compensation techniques have relied on feedback approaches to minimize system sensitivity and resulting response to narrowband disturbances. These approaches bring with them limitations such as limited stability margins and reduced robustness. Feedforward disturbance cancellation has the advantage that it remains stable, since only system zeros are being changed, and can be made easily adaptive for changing systems and environments. Such methods work quite well for narrow and wideband disturbances, however it should be noted that they do require compensators of large order for broadband disturbances. This work investigates the effect of using filtered-X LMS as a viable means of feedforward control for time-periodic systems. Later, Chapter 4 will provide a derivation of this algorithm.

2.5 Control Techniques Specific to Time-Periodic Systems

Recently, there has been some focus on controlling time-periodic systems in particular. Grasselli and Longhi mention several papers which address this issue [1988]. Periodic systems cannot be described in terms of classical transfer functions or time-invariant state transition matrices. Thus conventional classical and modern state-space control techniques cannot be applied to these systems. As a result, the techniques developed for time-invariant systems are being transformed into techniques useful for time-periodic systems as well. As is well known, however, many difficulties are encountered in developing consistent extensions to the nonstationary case. Previous efforts in applying modern feedback control to time-periodic systems have included the output feedback and pole placement techniques [Calise, *et al.*, 1992]. This section will discuss several of the recent advances in the area of disturbance rejection for time-periodic systems.

2.5.1 Output Feedback

The application of memoryless linear periodic output feedback has been shown to work for certain (controllable and observable) linear time-invariant discrete-time systems, resulting in exact pole-placement. Recent papers by Aeyels and Willems [1991, 1992] have discussed that this is possible for certain system conditions. Thus, it was only logical for them to explore the application of this controller to time-periodic systems. Their investigation concerns the general case of discrete systems. The major assumption in their controller is that the time-dependent feedback gain is periodic with the same period as the system, or a multiple thereof [Aeyels and Willems, 1995]. In addition, the

disturbance states must be augmented to the system states for both of these output feedback systems as explained in section 2.2.1 using equations 2.2.8 - 2.2.11 for disturbance rejection. After following these steps, the disturbance is then included in the new state dynamics matrix, \mathbf{A}_a , and the output feedback controller developed by Aeyels and Willems is then implemented. It should be noted that there is no discussion on the robustness of this algorithm, nor is any indication of its performance given.

A similar controller was developed by Calico and Wiesel [1984] previous to the work of Aeyels and Willems for time-periodic systems using output feedback. They implemented a linear quadratic Gaussian (LQG) controller in their analysis. This method involves solving a periodic Riccati equation and implementing periodic feedback gains. However, a LQG controller of this type requires that an observer with periodic filter gains be implemented in real time to estimate all of the unmeasured states. In addition, a negative effect of applying a LQG controller is that all the states are penalized equally over all frequencies. Many time-periodic systems have higher harmonic content due to the infinite number of higher frequency poles which could be of great significance. Typical linear quadratic Gaussian controllers penalize the states over all frequencies. Thus, unacceptably high feedback gains and bandwidth for the closed-loop system may result. For this reason, Calise, *et al.* [1992] developed a version of a LQG controller which penalizes the response and control envelope using Floquet-Lyapunov theory. This method enables the designer to distribute the performance penalty over certain frequencies of interest and to choose the state and control weighting matrices accordingly. However, the effort by Calise, *et al.* uses time-invariant feedback gains. Their results show reliable convergence with the application of their theory to the helicopter rotor blade in forward flight. Using position and rate information for in-plane dynamics, the control was found to be quite effective in minimizing vibrations for a blade

model which included both in-plane (lead-lag) and out-of-plane (flap) dynamics [Calise, *et al.*, 1992].

2.5.2 Pole Placement

Several efforts to control periodic systems via pole placement techniques have recently been published. Sreedhar and Van Dooren developed a technique which assigns the closed-loop characteristic multipliers [1993]. (Characteristic multipliers are the eigenvalues of $F = \Phi_A(t_0+T, t_0)$ where $\Phi_A(t, \cdot)$ is the transition matrix of \mathbf{A} .) However, this technique is very tedious and computationally elaborate due to the fact that the *precise* location of closed-loop poles is desired. For this reason, they further developed their technique for applications where the exact closed-loop pole location is unimportant. In this simple algorithm, the solution to a periodic Lyapunov equation is found. The solution “gives a number $0 < \alpha < 1$ such that all closed-loop poles have [a] magnitude less than α . Moreover, it works only with that sub-system whose poles need to be shifted, and is [computationally] cheaper than an explicit pole placement routine” [Sreedhar and Van Dooren, 1994]. The implementation of the two algorithms (Sreedhar and Van Dooren 1993, 1994) has two major drawbacks: 1) the computational inefficiency of the first may be too unreasonable to implement, and 2) the exact pole locations may be needed, especially for very sensitive systems. In addition, the disturbance states must be augmented to the system states for disturbance rejection here as well as shown in section 2.2.1.

2.5.3 Adaptive Control Via the Pulse Response Method

Since the response and disturbance input of a time-periodic system vary with time, an adaptive controller is ideally needed for control over all time. Knospe and Haviland [1991] have developed an adaptive controller which uses a cautious controller in the discrete-time domain. A pulse-response formulation, as opposed to a frequency-domain approach, is used to reduce the vibrations of a helicopter rotor blade at all harmonics (multiples of the blade passing frequency). A probing signal, or pseudorandom signal, is inserted into the control in order to bound the covariances and stabilize the system. This is needed due to the control not completely spanning the parameter space (i.e. not enough control authority exists otherwise). Results for the helicopter rotor blade problem typically show a vibration reduction of 15 dB when the probing signal is used. Results without using the probing signal show a slightly larger vibration reduction. Thus, “probing can prevent covariance instability due to insufficient richness of the control at the expense of a small loss in attenuation performance” [Knospe and Haviland, 1991].

2.5.4 Filtered-X LMS Algorithm

The next controller that we wish to discuss for controlling time-periodic systems is the filtered-X LMS algorithm. Research in this area has not previously been published and so this work presents the results for this adaptive controller. Before the filtered-X LMS algorithm can be applied to a time-periodic system, however, we must first derive the solution to its differential equation. A discrete state-space representation of a time-periodic system can then be written. After this is performed, the disturbance dynamics are

added to the system state dynamics matrix. At this point the adaptive algorithm can be applied to the system. In the following chapter these derivations will be shown.

Chapter 3

Time-Periodic Systems

There is a large class of linear equations whose coefficients are not constants, but instead functions of the independent variable. "Equations with variable coefficients may arise from physical systems in which some parameter is caused to vary with time because of the action of a process outside the system itself" [Cunningham, 1958]. This occurs in mechanical as well as electrical systems. For example, the capacitance of a condenser microphone varies in response to a sound wave striking the microphone. This varying capacitance leads to an electrical circuit with a varying parameter. Helicopter rotor blades flap in sinusoidal motion as a function of azimuth angle as they rotate around the rotor and translate through the air in forward flight. It is these types of time-periodic systems which are of interest to this work. Digital hardware is used to implement adaptive control to a system, and so first we must take the continuous time model of a system (known from dynamic equations, e.g. for the helicopter system, aerodynamic theory) and convert it to the discrete time domain.

This chapter will provide the generalized solution to a time-periodic differential equation. Included in this derivation is a method for augmenting the dynamics of a disturbance to the system states to facilitate disturbance rejection. The solution to the differential equation is then discretized. With the state-space model then readily determined, the adaptive controller to be used for control, the filtered-X LMS algorithm, will then be discussed in Chapter 4.

3.1 Solving Differential Equations with Time-Varying Coefficients

Modern control has thoroughly investigated how to solve systems of differential equations with constant coefficients. In addition, digital implementation of these techniques has been established and demonstrated. The solution to differential equations with time-varying parameters has also been investigated by many such as Chen [1984]. However, digital representation of these types of systems is much more difficult. In the next section, the well-established digital solution to systems with constant coefficients is discussed to provide a foundation for the sections that follow. The digital solution for systems with time-varying coefficients will be then analyzed. As we shall see, this solution presents many mathematical complexities for digitally implementing a system known in the continuous time domain.

3.1.1 Discrete State-Space Solution to Differential Equations with Constant Coefficients

The state-space representation of a system of ordinary differential equations is of the form

$$\dot{\mathbf{x}} = \mathbf{Ax} + \mathbf{Bu} \quad (3.1.1)$$

$$\mathbf{y} = \mathbf{Cx} + \mathbf{Du} \quad (3.1.2)$$

where \mathbf{x} is the state vector, \mathbf{u} is the input, and \mathbf{y} is the output vector. (Ignore any disturbance inputs for the time being.) The matrices \mathbf{A} , \mathbf{B} , \mathbf{C} , and \mathbf{D} do not vary with time here. To solve this differential equation, we assume a solution for the homogenous part of

equation 3.1.1. That is, we solve for the solution where \mathbf{u} is equal to zero. The assumed solution, called $\mathbf{x}_h(t)$, spans the space of all possible solutions and is defined as

$$\dot{\mathbf{x}}_h = \mathbf{A}\mathbf{x}_h(t) ; \mathbf{x}_h(t_0) = \mathbf{x}_0 \quad (3.1.3)$$

and results in the solution

$$\mathbf{x}_h(t) = e^{\mathbf{A}(t-t_0)}\mathbf{x}(t_0) \quad (3.1.4)$$

Next, we use variation of parameters to solve for the non-homogenous or particular solution. The following guess is made:

$$\mathbf{x}_p(t) = e^{\mathbf{A}(t-t_0)}\mathbf{v}(t) \quad (3.1.5)$$

Substituting equation 3.1.5 into 3.1.1 and integrating yields

$$\mathbf{v}(t) = \int_{t_0}^t e^{-\mathbf{A}(\tau-t_0)}\mathbf{B}\mathbf{u}(\tau)d\tau \quad (3.1.6)$$

Substituting this back into equation 3.1.5 and using the following relations,

$$e^{\mathbf{A}(t_2-t_0)} = e^{\mathbf{A}(t_2-t_1)}e^{\mathbf{A}(t_1-t_0)} \quad (3.1.7)$$

we obtain the final form of the particular solution:

$$\mathbf{x}_p(t) = \int_{t_0}^t e^{\mathbf{A}(t-\tau)}\mathbf{B}\mathbf{u}(\tau)d\tau \quad (3.1.8)$$

The total solution then becomes

$$\mathbf{x}(t) = \mathbf{x}_h(t) + \mathbf{x}_p(t) = e^{\mathbf{A}(t-t_0)}\mathbf{x}(t_0) + \int_{t_0}^t e^{\mathbf{A}(t-\tau)}\mathbf{B}\mathbf{u}(\tau)d\tau \quad (3.1.9)$$

We must now discretize this solution by letting $t = kT+T$ and $t_0 = kT$, where T is the sample period. Equation 3.1.9 then becomes

$$x(kT + T) = e^{AT} x(kT) + \int_{kT}^{kT+T} e^{A(kT+T-\tau)} \mathbf{B}u(\tau) d\tau \quad (3.1.10)$$

Making a change of variable $\tau = kT + T - \eta$ and considering a zero-order hold such that $u(\tau) = u(kT)$ over the interval results in

$$x(kT + T) = e^{AT} x(kT) + \int_0^T e^{A\eta} \mathbf{B}u(kT) d\eta \quad (3.1.11)$$

Including a disturbance as one of the inputs, this relation is then commonly written as

$$x(k + 1) = \Phi x(k) + \Gamma u(k) + \Gamma_1 d(k) \quad (3.1.12)$$

where

$$\Phi = e^{AT} \quad \text{and} \quad \Gamma_1 = \int_0^T e^{A\eta} \mathbf{B} d\eta \quad (3.1.13)$$

$\Gamma_1 = \Gamma \mathbf{D}$ with \mathbf{B} replaced by the input matrix of the disturbance if the disturbance, \mathbf{d} , is a constant. If \mathbf{d} is an impulse, $\Gamma_1 = \Gamma$ input matrix of the disturbance. Otherwise, Γ_1 becomes more complicated [Franklin, Powell, and Workman, 1990]. These variables in equation 3.1.13 are then used in the digital control application of interest. Standard digital control algorithms have been developed for this type of system based on equations 3.1.12 and 3.1.13 above. However, when the coefficients are instead time-varying, representation in the digital domain is quite different.

3.1.2 Discrete State-Space Solution to Differential Equations with Time-Varying Coefficients

The transformation of a time-varying continuous system into the discrete domain complicates the procedure just discussed, which led to the convenient formula in 3.1.12

and 3.1.13. The arrival at the assumed homogeneous solution in equation 3.1.3 involved a few assumptions which we shall now discuss.

In assuming equation 3.1.4 as the homogeneous solution to the differential equation, we are in effect assuming that there exists a smooth solution so that a series expansion of the solution is possible. In other words, it assumes that

$$x_h(t) = \mathbf{F}_0 + \mathbf{F}_1(t - t_0) + \mathbf{F}_2(t - t_0)^2 + \dots \quad (3.1.14)$$

where \mathbf{F}_i are arbitrary matrices. Letting $t = t_0$ results in $\mathbf{F}_0 = \mathbf{x}_0$. Differentiating again and again results in expressions for $\mathbf{F}_1, \mathbf{F}_2, \mathbf{F}_3, \dots$ etc. [Franklin, *et al.*, 1990]. This leads to the following equation:

$$x_h(t) = [\mathbf{I} + \mathbf{F}(t - t_0) + \frac{\mathbf{F}^2(t - t_0)^2}{2} + \frac{\mathbf{F}^3(t - t_0)^3}{6} + \dots] \mathbf{X}_0 \quad (3.1.15)$$

The application of this technique to time-varying systems fails here in the differentiation of the power series. Since all the terms are time-varying, the result shown in equation 3.1.15 will differ from that derived for systems with time-varying coefficients. We must therefore derive a new method to handle time-periodic systems.

We proceed as we did for the constant coefficient system by first assuming a solution for the homogenous part of equation 3.1.1. The assumed solution, called $\mathbf{x}_h(t)$, is

$$x_h = \mathbf{X}_0 e^{\mathbf{P}(t)} ; \dot{\mathbf{P}}(t) = \mathbf{A}(t) \quad (3.1.16)$$

This can also be represented by

$$x_h(t) = e^{\int_{t_0}^t \mathbf{A}(\tau) d\tau} \mathbf{X}_0 \quad (3.1.17)$$

Using variation of parameters to solve for the non-homogenous or particular solution, the following guess is made:

$$x_p(t) = \mathbf{Q} e^{\mathbf{P}(t)} v(t) \quad (3.1.18)$$

Substituting equation 3.1.18 into 3.1.1 and integrating yields

$$v(t) = \frac{1}{\mathbf{Q}} \int_{t_0}^t e^{-\mathbf{P}(\tau)} \mathbf{B}(\tau) u(\tau) d\tau \quad (3.1.19)$$

Substituting this back into equation 3.1.18 we obtain the final form of the particular solution:

$$x_p(t) = e^{\int_{t_0}^t \mathbf{A}(\tau) d\tau} \int_{t_0}^t e^{-\int_{t_0}^{\tau} \mathbf{A}(\zeta) d\zeta} \mathbf{B}(\tau) u(\tau) d\tau \quad (3.1.20)$$

The total solution then becomes

$$x(t) = x_h(t) + x_p(t) = e^{\int_{t_0}^t \mathbf{A}(\tau) d\tau} \mathbf{X}(t_0) + e^{\int_{t_0}^t \mathbf{A}(\zeta) d\zeta} \int_{t_0}^t \mathbf{B}(\tau) u(\tau) d\tau \quad (3.1.21)$$

Comparing this to equation 3.1.9, we see that both the homogeneous and particular portions of the solution differ. We can not easily discretize equation 3.1.21 into a useful form.

For modeling algorithms, for example, equation 3.1.21 cannot be easily implemented for a time-varying input, such as a sinusoidal disturbance input. This is because equation 3.1.21 cannot be put in the form of equation 3.1.12 due to the fact that the input is in the integral term. For time-varying inputs, we must instead augment the states of the system such that the resulting new 'input' is a constant. This method will be discussed in the following section.

3.2 Disturbance Models Using Augmented States

To alleviate the problems just discussed, we must augment the system states to include the disturbance input. This is done as explained in Chapter 2 using equations 2.2.8 - 2.2.11. After following those steps, the time-varying disturbance dynamics are then

included in the new state dynamics matrix, \mathbf{A}_a , and the formulation found in equation 3.1.21 can be used with minor modification:

$$x(t) = e^{\int_{t_0}^t \mathbf{A}_a(\tau) d\tau} \mathbf{X}(t_0) + \int_{t_0}^t e^{\int_{\tau}^t \mathbf{A}_a(\tau) d\tau} \mathbf{B}_a(\tau) u(\tau) d\tau \quad (3.2.1)$$

Now the input \mathbf{u} contains only the control input, which, if generated with a zero-order hold, is constant over the sampling period. Thus, as we did for the constant coefficient system, we can assume a zero-order hold on the input such that $u(\cdot) = u(kT)$. The input can then be pulled out of the integral, and discretization occurs as in the time-invariant system formulation by letting $t = kT + T$ and $t_0 = kT$. Equation 3.2.1 can thus be solved, although with much tedious integration. Equation 3.1.12 is then obtained where

$$= e^{\int_{kT}^{kT+T} \mathbf{A}_a(\tau) d\tau} \quad \text{and} \quad = \int_{kT}^{kT+T} e^{\int_{\tau}^{kT+T} \mathbf{A}_a(\zeta) d\zeta} \mathbf{B}_a(\tau) u(\tau) d\tau \quad (3.2.2)$$

For this case, $\mathbf{d}_1 = 0$ since the disturbance d has been incorporated into \mathbf{u} .

Chapter 4

Adaptive Control

Filtered-X LMS, the controller used in this investigation, is a subset of a technique called adaptive filtering. This is a feedforward technique which involves canceling a disturbance from a system's response with a reference input. Cancellation is achieved by first passing the reference input through a filter whose parameters are adjusted in such a way that the resulting signal will eliminate the effects of the disturbance on the system [Widrow, 1985]. The following sections will describe the basics of adaptive filtering, the least-mean-square algorithm, and the steps needed to derive the filtered-X LMS algorithm.

4.1 Adaptive Filtering

The adaptive linear combiner, or nonrecursive adaptive filter is typically employed in adaptive filtering. This is a finite impulse response (FIR) digital filter and is shown in Figure 4.1.

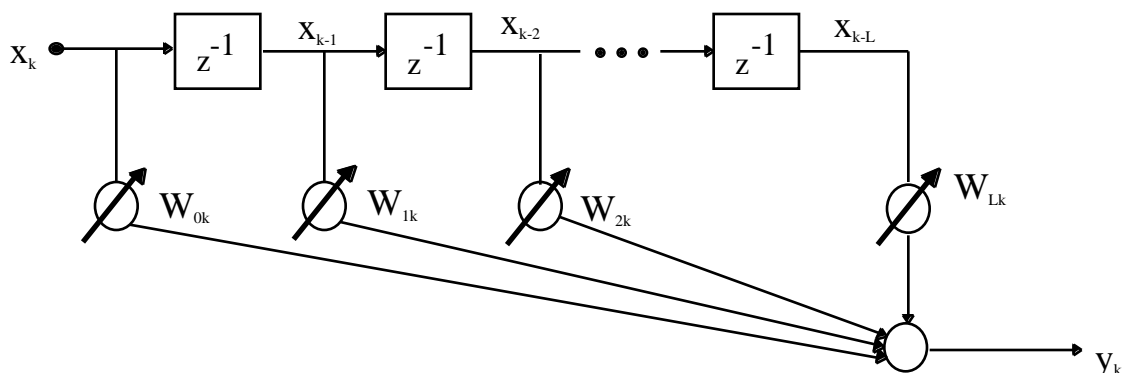


FIGURE 4.1 Single-Input Adaptive Transversal Filter

In this discrete implementation the z^{-1} refers to a delay of one time step. This is known as a tap delay line and its transfer function can be written as

$$H(z) = w_0 + z^{-1}w_1 + \dots + z^{-L}w_L \quad (4.1.1)$$

For this investigation, there is a single input with $L+1$ sequential samples such that

$$\bar{\mathbf{X}}_k = [\mathbf{x}_k \ \mathbf{x}_{k-1} \ \mathbf{x}_{k-2} \ \dots \ \mathbf{x}_{k-L}]^T \quad (4.1.2)$$

$$\mathbf{w}_k = [w_{0k} \ w_{1k} \ \dots \ w_{Lk}] \quad (4.1.3)$$

The output of the block diagram in the figure then becomes

$$y(k) = \sum_{l=0}^L w_{lk}x_{k-l} \quad (4.1.4)$$

A typical use for such an adaptive algorithm is shown in Figure 4.2. This figure shows a system in which an adaptive algorithm is used to adjust the adaptive filter such that the output y_k is equal to the reference input, r_k , thus driving the error, e_k , to zero.

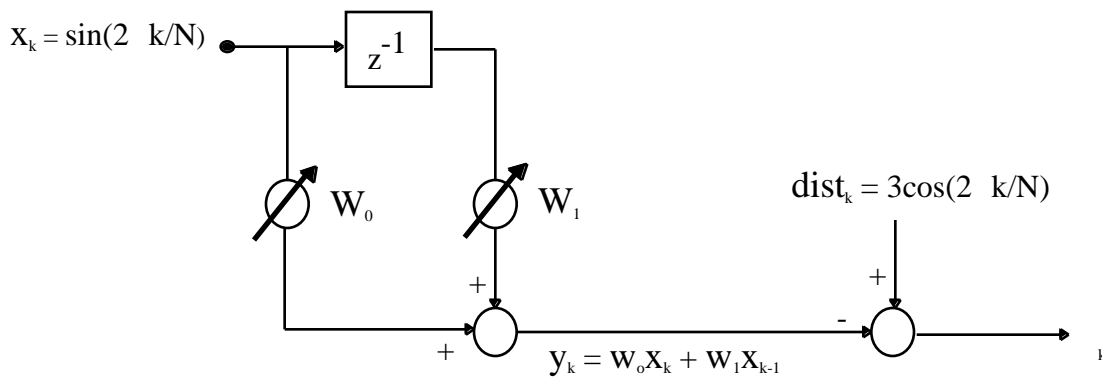


FIGURE 4.2 Example of an Adaptive Linear Combiner [Widrow, 1985]

Adaptive algorithms must have a performance function which defines what variable should be minimized. The algorithm used in this study minimizes the error signal, ε_k according to the following equation

$$\varepsilon_k = d_k - y_k \quad (4.1.5)$$

where d_k is the desired response. Given equation 4.1.4, this becomes

$$\varepsilon_k = d_k - \mathbf{X}_k^T \mathbf{W}_k \quad (4.1.6)$$

Squaring terms we obtain

$$\varepsilon_k^2 = d_k^2 + \mathbf{W}^T \mathbf{X}_k \mathbf{X}_k^T \mathbf{W} - 2d_k \mathbf{X}_k^T \mathbf{W} \quad (4.1.7)$$

Assuming ε_k , d_k , \mathbf{X}_k are *statistically stationary* and \mathbf{W} is constant (weights are not adaptive or are slowly changing compared to the other variables), we take the expected value of (4.1.7) over k to find the mean-square error:

$$E[\varepsilon_k^2] = E[d_k^2] + \mathbf{W}^T E[\mathbf{X}_k \mathbf{X}_k^T] \mathbf{W} - 2E[d_k \mathbf{X}_k^T] \mathbf{W} \quad (4.1.8)$$

We now define the input correlation matrix, \mathbf{R} , as

$$\mathbf{R} = E[\mathbf{X}_k \mathbf{X}_k^T] \quad (4.1.9)$$

and the column vector of cross correlations between the input components and the desired response as

$$\mathbf{P} = E[d_k \mathbf{X}_k] \quad (4.1.10)$$

Renaming the mean-square error as ξ , equation (4.1.8) becomes

$$MSE \quad \xi = E[\varepsilon_k^2] = E[d_k^2] + \mathbf{W}^T \mathbf{R} \mathbf{W} - 2\mathbf{P}^T \mathbf{W} \quad (4.1.11)$$

Thus the mean-square error is a quadratic function in \mathbf{W} given the assumption of the statistical stationarity of variables ε_k , d_k , \mathbf{X}_k . The performance surface defined by the mean-square error function is a paraboloid (or hyperparaboloid for more than two

weights). The adaptive algorithm adjusts the weights until the optimal weight vector is achieved, \mathbf{W}^* . At this point the mean-square error is at its global minimum and the system operates at the "bottom of the mean-square error bowl." No local minima exist for this performance surface.

There are many different adaptive systems that cause the weight vector to seek the minimum of the performance surface by means of gradient methods. The gradient of the mean-square error can be obtained by differentiating (4.1.11) to obtain

$$\frac{\partial \xi}{\partial \mathbf{W}} = 2\mathbf{R}\mathbf{W} - 2\mathbf{P} \quad (4.1.12)$$

To get the minimum mean-square error, \mathbf{W} is set at its optimal value \mathbf{W}^* as just mentioned:

$$= \bar{\mathbf{0}} = 2\mathbf{R}\mathbf{W} - 2\mathbf{P} \quad (4.1.13)$$

Assuming \mathbf{R} is nonsingular, the optimal solution, called the Wiener solution, is

$$\mathbf{W} = \mathbf{R}^{-1}\mathbf{P} \quad (4.1.14)$$

After some massaging, the minimum mean-square error of (4.1.11) becomes

$$\xi_{\min} = E[d_k^2] - \mathbf{P}^T \mathbf{R}^{-1} \mathbf{P} = E[d_k^2] - \mathbf{P}^T \mathbf{W} \quad (4.1.15)$$

Two well-known adaptive algorithms used to achieve this minimum are the method of steepest descent and Newton's method. Both of these methods use the gradient of the mean-square error to determine the direction of surface's minimum. Newton's method is significant historically, however it is often difficult to implement in practice. In addition, the method can be reduced to one which has one-step convergence. In general, this is undesirable because usually \mathbf{R} is unknown and must be estimated or measured on the basis of stochastic input data. A slow adaptation process diminishes the effects of gradient measurement noise. Thus, the one-step Newton's method is impractical. The

method of steepest descent is used in this study and so Newton's method will not be discussed hereafter.

The algorithm for the method of steepest descent may be written as

$$\mathbf{W}_{k+1} = \mathbf{W}_k + \mu(-\nabla J_k) \quad (4.1.16)$$

where μ is a constant which regulates the step size and has the dimensions of inverse signal power. It regulates the speed and stability of the adaptation process as well as the noise in the weight vector. The noise is attenuated by the adaptive process which acts like a low-pass filter. Defining a deviation vector

$$\mathbf{V} = \mathbf{W} - \mathbf{W} \quad (4.1.17)$$

and using (4.1.13), the algorithm of (4.1.16) becomes

$$\mathbf{W}_{k+1} = \mathbf{W}_k + 2\mu\mathbf{R}(\mathbf{W} - \mathbf{W}_k) = (\mathbf{I} - 2\mu\mathbf{R})\mathbf{W}_k + 2\mu\mathbf{R}\mathbf{W} \quad (4.1.18)$$

The solution to this equation is complicated due to the cross-coupling of the components of \mathbf{W} (since \mathbf{R} is not diagonal in general). For this reason, the derivation of the solution shown in equation 4.1.19 may be found in Widrow [1985]:

$$\mathbf{W}_k = \mathbf{W} + (\mathbf{I} - 2\mu\mathbf{R})^k (\mathbf{W}_0 - \mathbf{W}) \quad (4.1.19)$$

4.2 Least-Mean-Square Algorithm

In the adaptive filter equations of the previous section the algorithm minimized $\xi = E[\varepsilon_k^2]$. However, the least-mean-square (LMS) algorithm minimizes $\xi = \varepsilon_k^2$. This is convenient because there is no averaging and thus the LMS algorithm is simple and

efficient. Taking differences between short-term averages of ϵ_k^2 and using (4.1.6), the gradient estimate becomes

$$\hat{\mathbf{g}}_k = \begin{bmatrix} \frac{\partial \epsilon_k^2}{\partial w_0} \\ \vdots \\ \frac{\partial \epsilon_k^2}{\partial w_L} \end{bmatrix} = 2\epsilon_k \begin{bmatrix} \frac{\partial \epsilon_k}{\partial w_0} \\ \vdots \\ \frac{\partial \epsilon_k}{\partial w_L} \end{bmatrix} = -2\epsilon_k \mathbf{X}_k \quad (4.2.1)$$

The LMS algorithm uses the steepest descent method to minimize the mean-square error so that (4.1.16) becomes

$$\mathbf{W}_{k+1} = \mathbf{W}_k + 2\mu\epsilon_k \mathbf{X}_k \quad (4.2.2)$$

The optimal solution is again found to be the Wiener equation of (4.1.14).

A primary concern with the algorithm is convergence. By taking the expected value of (4.2.2) and changing the coordinate system we find the following inequality which guarantees convergence

$$\frac{1}{\lambda_{\max}} > \mu > 0 \quad (4.2.3)$$

where λ_{\max} is the largest eigenvalue of the eigenvalue matrix Λ , where $\mathbf{RQ}=\mathbf{Q}\Lambda$. It is generally easier to determine the elements of \mathbf{R} rather than the eigenvalues of \mathbf{R} . A simpler but more restrictive bound on μ is

$$0 < \mu < \frac{1}{tr[\mathbf{R}]} \quad (4.2.4)$$

4.3 Adaptive Inverse Control

The adaptive inverse control problem “was developed to accommodate situations where the plant might be ‘non-minimum-phase,’ that is, might have transfer function zeros in

the right half of the s-plane” [Widrow, 1985]. Its development is a precursor to understanding the filtered-X LMS algorithm which will be discussed in the subsequent section. For this reason, a discussion of adaptive inverse control follows.

The idea behind inverse control is quite simple: any [un]known plant can be made to track a reference command signal when the signal is applied to a controller whose transfer function is the inverse of that of the plant. The controller’s transfer function is determined through adaptive inverse modeling techniques applied to the plant. Figure 4.3 shows how this model is formed.

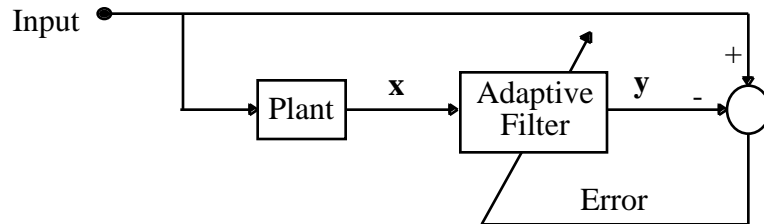


FIGURE 4.3 Inverse Plant Modeling

The equation defining the adaptive filter is

$$\mathbf{y} = \mathbf{W}^T \mathbf{x} \quad (4.3.1)$$

The filter is adapted until its output is the minimum mean-squared match of the plant input [Widrow, 1985].

Noise present in most systems can be represented as an additive effect at the plant’s output. The effects of unwanted noise on the performance of an adaptive inverse model are shown in Figure 4.4.

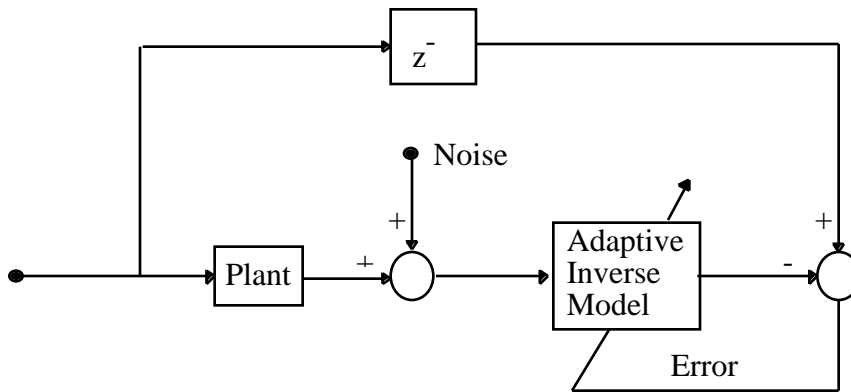


FIGURE 4.4 Adaptive Inverse Modeling of a Noisy Plant

The noise presents problems in the adaptive inverse modeling algorithm because the noise is uncorrelated (in general) with the input to the system. As the adaptive process converges, the inverse model approaches the Wiener solution $\mathbf{R}^{-1}\mathbf{P}$ from equation (4.1.14). The noise will effect the control weighting matrix \mathbf{R} and therefore \mathbf{R}^{-1} as well. This will result in an error in the adaptive solution; the inverse model will, in general, be different from the desired delayed inverse model. Therefore, this adaptive inverse control method will not be practical if there is significant noise in the system [Widrow, 1985].

4.4 Filtered-X LMS For Disturbance Rejection

The filtered-X LMS algorithm is an adaptation of the inverse model previously discussed. Its development was a result of attempting to eliminate the effects of noise on the adaptive inverse model. This is accomplished by preventing the noise from being an input to the adaptive inverse model. The noise will still have an effect on the error, but it will

not have an impact on the converged solution of the adaptive model. Implementation of this algorithm is shown in Figure 4.5.

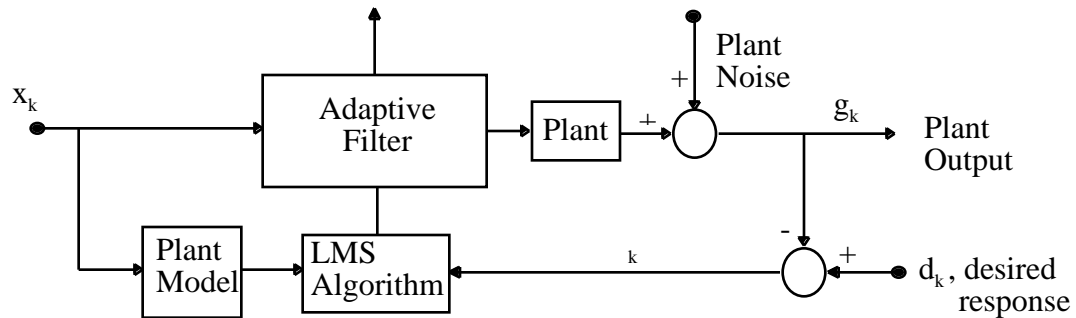


FIGURE 4.5 Filtered-X LMS Algorithm

By filtering the reference input x_k , convergence and stability problems are improved from the original LMS algorithm configuration [Widrow, 1985]. The reference signal is applied to both the plant model and the adaptive filter. Since there is a delay as the reference signal makes its way through to the output of the plant, a model of the plant must be incorporated into the lower loop. This prevents the error signal entering the LMS algorithm from being improperly phased with the reference input at any instant in time so that proper adjustment of the weights in the filter can occur.

Figure 4.6 shows a detailed block diagram of the filtered-X LMS controller.

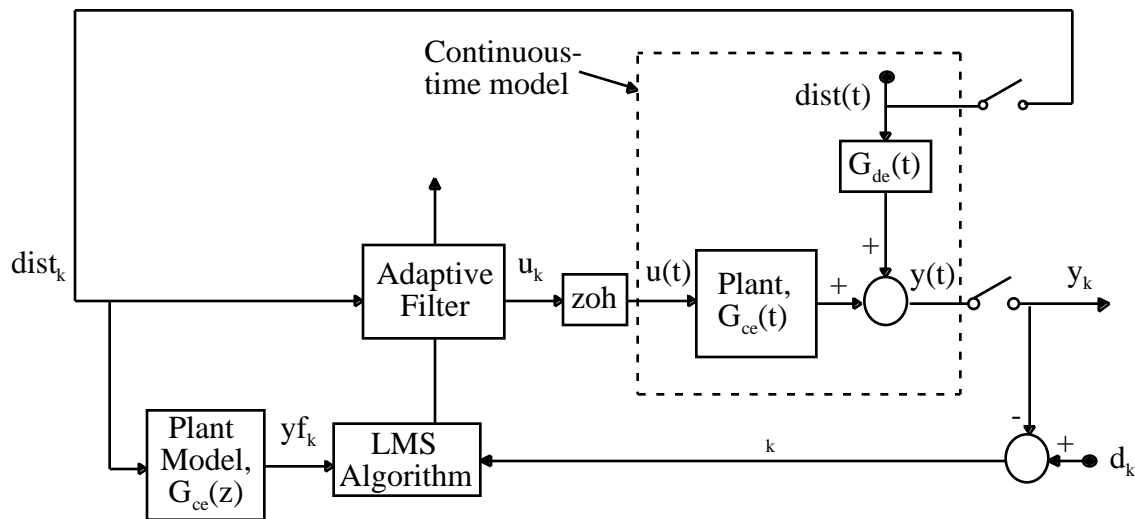


FIGURE 4.6 Filtered-X LMS Controller for Generalized Time-Periodic System

In this diagram, the plant represents the control to error path, and the disturbance enters through the disturbance to error path, which is generally unknown in most systems. The area enclosed in the dotted line is then the continuous-time model, or the augmented model of the system. In this augmented model the disturbance is one of the states. It can therefore be fed back to the input of the adaptive filter and the input of the plant model. The plant model contains only the dynamics of the original plant, without the augmented disturbance states. This is because this discrete transfer function is simply a model of the plant, or the control to error path. The variable d_k in Figure 5.1 is the desired response, equal to zero for this case.

A couple of crucial assumptions were made in developing the filtered-X LMS algorithm which should be mentioned. The transfer function of the plant is commutable with the adaptive filter only if the plant is linear and “if time variations of the impulse responses of both the plant and the adaptive filter take place with time constants long compared to the combined memory times or time constants of the adaptive filter and the

plant.” Therefore slow adaptation is required in order to satisfy these conditions. With these restrictions established however, it can be shown that the “expected value of the weight vector is unaffected by independent plant noise.” The only effects of the noise will be an additional misadjustment in the weight vector [Widrow, 1985]. Misadjustment is the ratio of the excess mean-square error over the minimum mean-square error, where excess MSE is defined as

$$excess\ MSE = E[\xi_k - \xi_{min}] \quad (4.4.1)$$

It should also be noted that the plant model shown in Figure 4.6 is usually implemented by an adaptive filter whose weights are found using an inverse modeling algorithm as discussed in section 4.3.

4.5 Algorithm Considerations for Time-Varying Systems

The Wiener solution derived in equation 4.1.14 has some interesting interpretations for time-varying systems. It is tempting to call it the Wiener solution for these types of systems as well. However, this is a misnomer since the nonstationary nature of the problem invalidates assumptions made in its derivation [Widrow and Walach, 1984]. Namely, the assumption made in section 4.1 that ξ_k is statistically stationary and \mathbf{W} is constant does not hold. For time-varying systems the signals are nonstationary and have statistical properties that vary with time. Thus the performance surface described by and the weights \mathbf{W} is moving in its coordinate system. The adaptive process then consists not only of moving downhill to the minimum, but also of tracking the minimum as it moves about the coordinate system. These effects have some interesting and complicated implications which we shall discuss in the following chapter as it pertains to the two systems investigated here.

Chapter 5

Filtered-X LMS for Linear Time-Periodic Systems

The development of the discretization of a continuous time-periodic system in Chapter 3 and the derivation of the filtered-X LMS algorithm in Chapter 4 have been used to examine two systems. The first is a generalized time-periodic system and the latter is the helicopter rotor blade in forward flight. This chapter investigates the performance of the filtered-X LMS algorithm in rejecting disturbances for these two systems.

5.1 Generalized Time-Varying System

The first application of filtered-X LMS for disturbance rejection investigated here is for a generalized time-periodic system. First the system will be described and then the results will be discussed. General trends regarding the influence of algorithm parameters such as the number of weights and μ will be investigated as well.

5.1.1 Equation of Motion

The equation of motion for the first-order generalized system is

$$\dot{x}(t) + (a_1 + a_2 \sin \omega t)x(t) = bu(t) + (d_1 + d_2 \sin \omega t) \quad (5.1.1)$$

where $d_1+d_2\sin t = \text{dist}(t)$ is the disturbance input, u is the control input, and x is the state. The disturbance states were first augmented to the system states; \mathbf{A}_d and \mathbf{C}_d are defined as

$$\mathbf{A}_d = \begin{bmatrix} 0 & 1 & 0 \\ 0 & 0 & 1 \\ 0 & -\omega^2 & 0 \end{bmatrix} \quad (5.1.2)$$

$$\mathbf{C}_d = [1 \ 0 \ 0] \quad (5.1.3)$$

The system was then discretized to form the discrete-time state-space model of the system as defined in equations 3.1.1 and 3.1.2. The filtered-X LMS controller was then applied to the system. Using 4 weight vectors and a convergence parameter of $\mu = 8e-2$, the following results were obtained. Note that the sampling frequency was 200 Hz whereas system frequency had a periodicity of 7 Hz.

Figure 5.1 shows a comparison between the open- and closed-loop error time responses. Note the periodic nature of both responses in the steady-state — this is a result of the time-varying nature of the system dynamics. The amplitude of the error is reduced from the open-loop system by 24.4 % (after convergence). In addition, the large bias error is almost completely eliminated.

Figures 5.2 and 5.3 show the control input and weight vectors respectively.

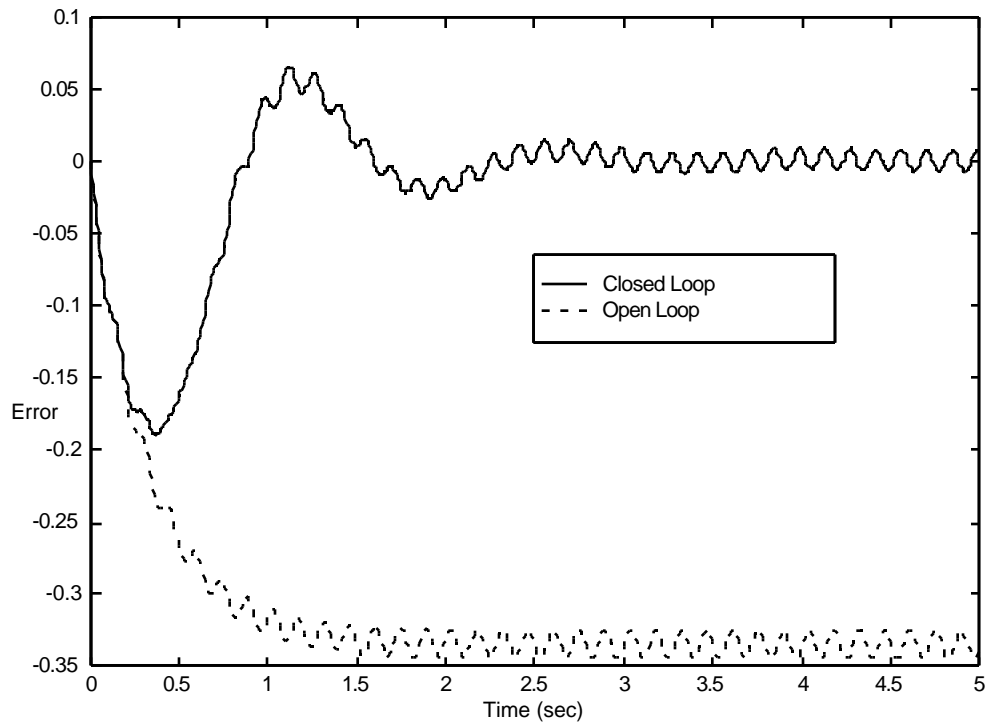


FIGURE 5.1 Error Time Response for Generalized System

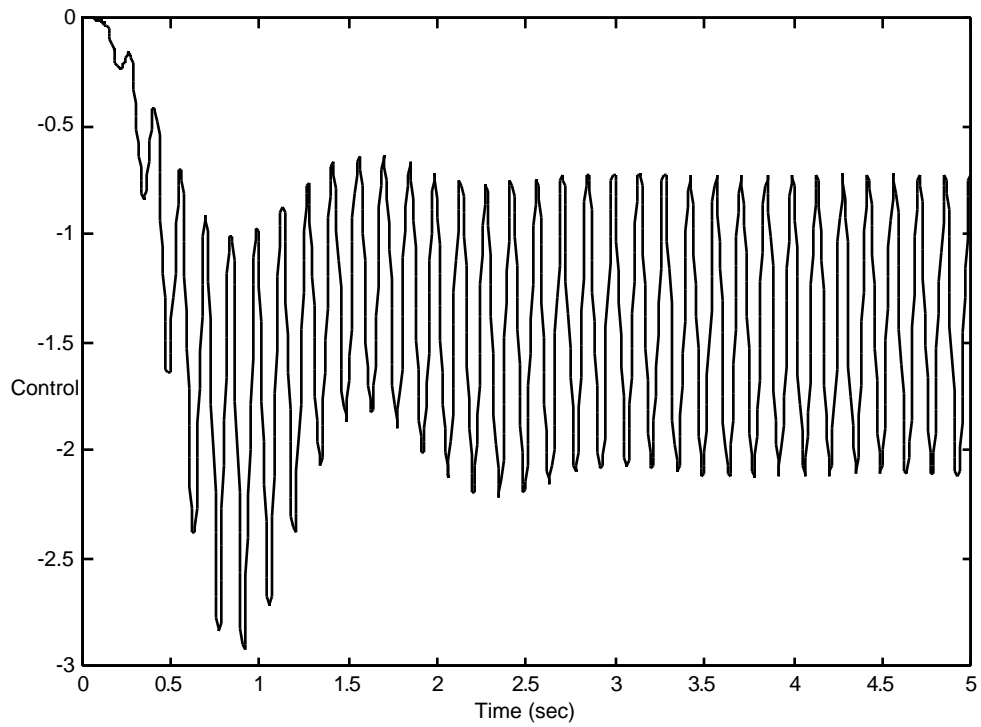


FIGURE 5.2 Control Input Time Response for Generalized System

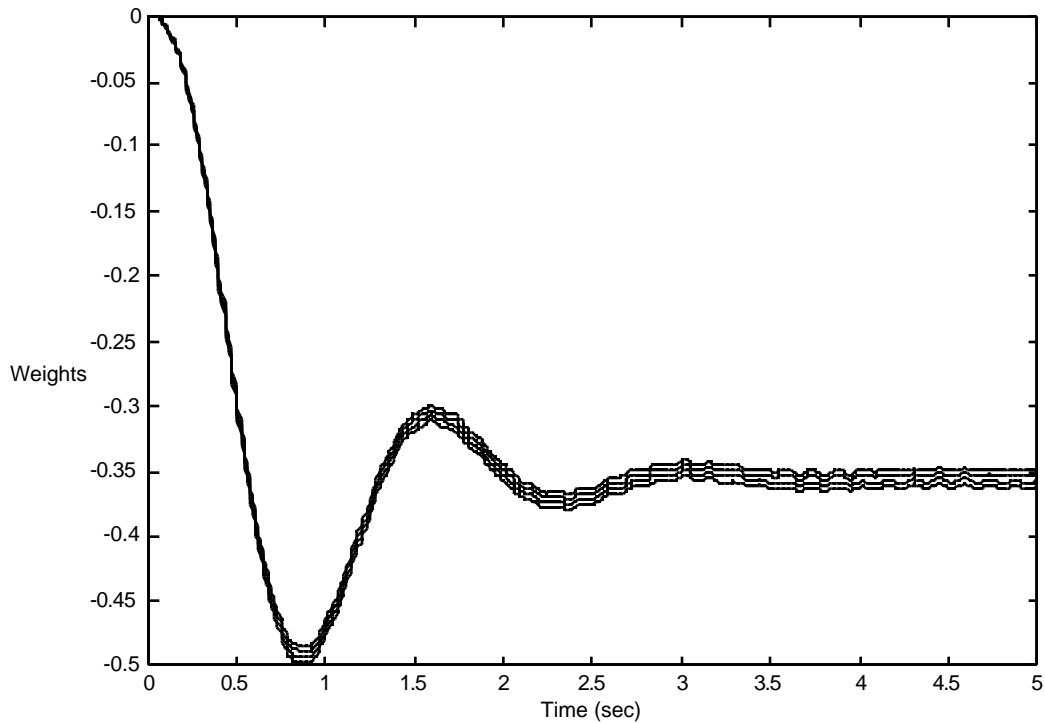


FIGURE 5.3 Weight Vector Time Responses for Generalized System

These plots show that the algorithm was able to converge, resulting in an error which oscillates generally about zero.

Several parameters were found to greatly affect the performance of the algorithm. Among them are the convergence parameter μ , the number of weights, and the sampling rate. The following sections will discuss the effects each of these parameters had on the controller's performance. Then a discussion of the overall performance of the algorithm on this generalized time-periodic system will follow.

5.1.2 Effect of the Convergence Parameter μ

It is well understood that μ has an upper bound, as defined in equation 4.2.3, in order to satisfy convergence requirements for linear time-invariant systems. The lower bound for this criteria is zero. However, for time-periodic systems the convergence parameter must be large enough such that the weights can adapt at least as fast as the system's periodicity. So the lower bound on μ for time-varying systems will be a value larger than zero. A plot of the optimal μ for a given cost function can be performed holding all other parameters fixed.

Figure 5.4 shows a plot of cost function E versus μ where E is the summation of the error, e , for the last ten iterations of the algorithm. Eight weights were used in this example. The system coefficients for this example were the following: $a_1 = .07$; $a_2 = 1$; $b = 1$; $d_1 = 2$; $d_2 = 1$; $w = 2$ (.08); $T_{\text{sample}} = 1/30$.

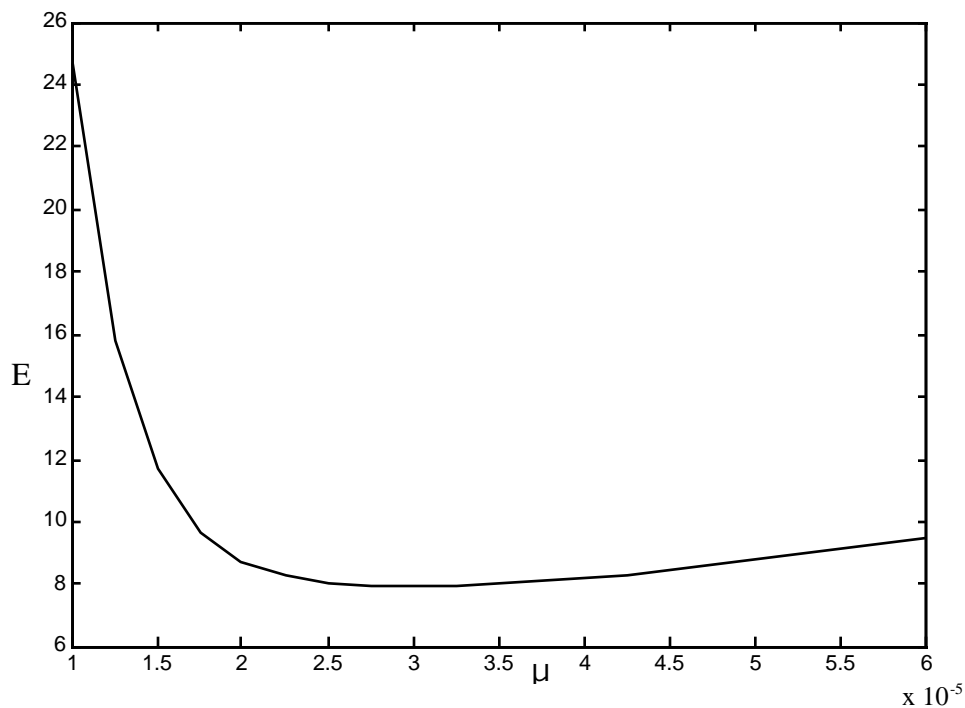


FIGURE 5.4 E versus μ , 8 Weights

Thus the optimal value of μ for the parameters given is approximately $2.8e^{-5}$. Any value of μ larger or smaller than this will result in excess mean-square error. This type of evaluation for an optimal μ can be performed in the final stages of any filtered-X LMS algorithm implementation to decrease the mean-square error and decrease the number of iterations until convergence as much as possible.

5.1.3 Effect of the Number of Adaptive Weights

In general, there is a minimum number of adaptive weights which must be used in order for the algorithm to converge. In other words, if less than the minimum number of weights is used there will not be enough control authority and thus the error will not converge to zero but will instead become infinitely large. This minimum number of weights to produce zero error can be found analytically if necessary. (Section 5.3 demonstrates this analysis for a second order system.) In addition, it seems likely that there may be some ideal number of weights just as there was an ideal value for μ . If more than the ideal number is used, no further benefit in algorithm performance will be realized. In addition, we shall also learn some additional effects of the convergence parameter μ as we look at the effects of the number of weights.

Using the same coefficients as the system described in section 5.1.2, the following E versus μ graph is obtained for 4 weights.

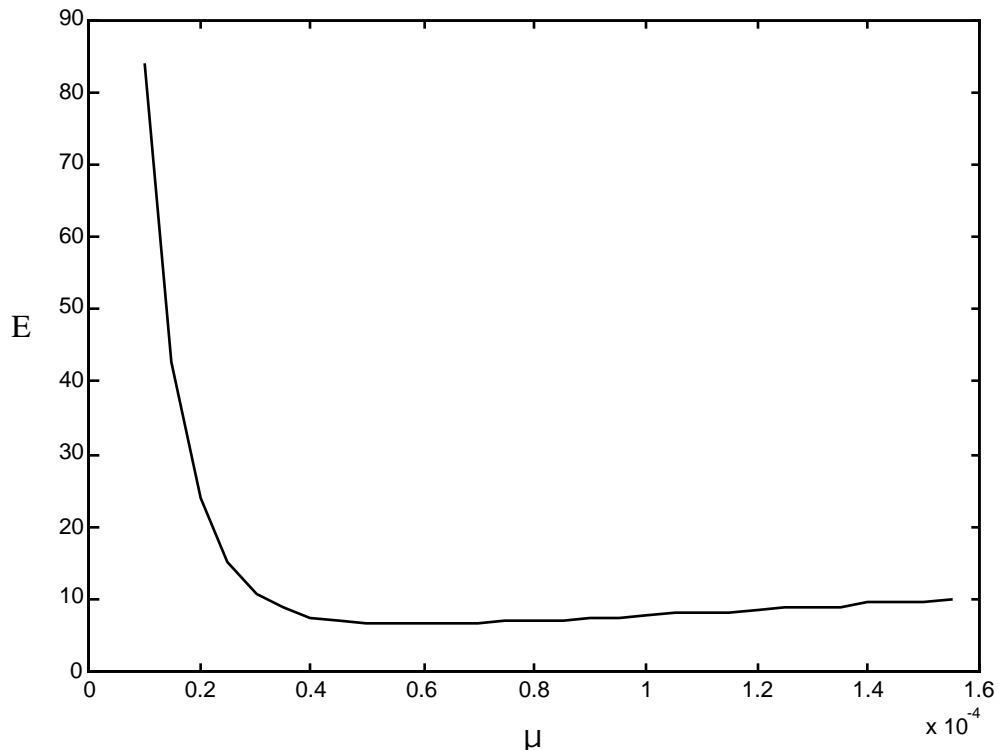


FIGURE 5.5 E versus μ , 4 Weights

So we can see that for fewer adaptive weights, the resulting optimal μ is about $5e-5$ — larger than the optimal μ found for the same system with twice as many weights.

Thus the effects of μ and the number of weights have opposite effects on one another — as the number of weights is increased, the system must adapt more slowly, resulting in a smaller optimal convergence parameter, μ . Similarly, as the number of weights decreases as shown in Figure 5.5, the system can adapt faster and so a larger μ can be tolerated. So for a given convergence parameter, one cannot say that a 16 weight filter is better than a 4 weight filter. Just the opposite may be true. But if μ is reduced for the filter with more weights, there may be fewer oscillations and smaller amplitudes of oscillation in the error response after convergence than that of the filter with less weights.

Figure 5.6 compares the error response for a system using both 16 and 4 weights versus the open-loop response to illustrate this scenario. μ is the same for both cases.

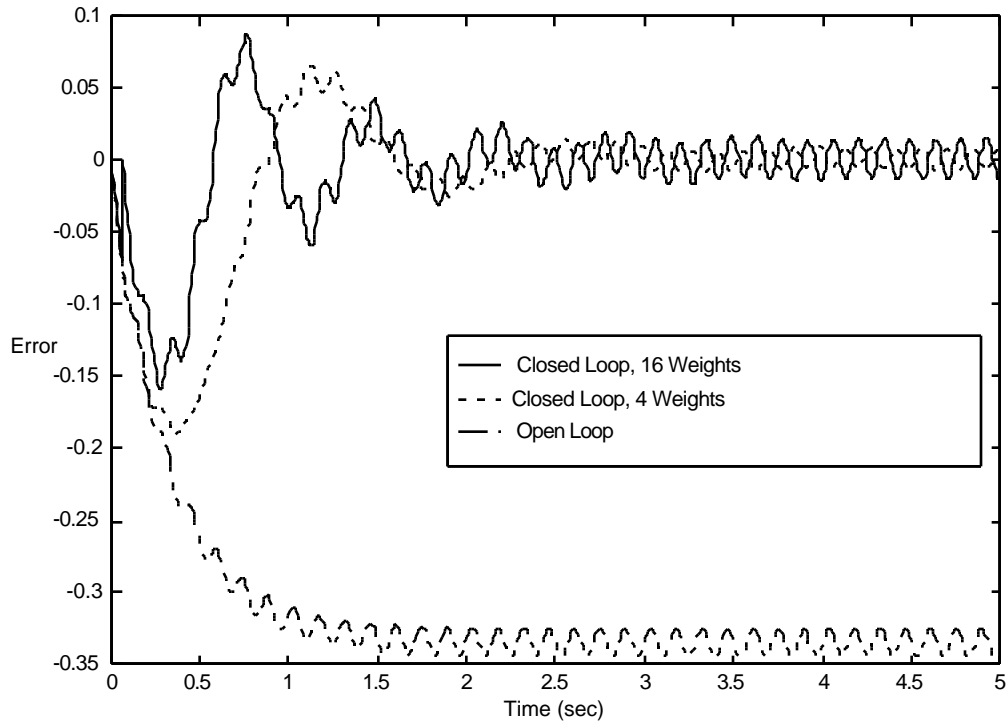


FIGURE 5.6 Comparison of Error Responses for Varying Number of Adaptive Weights and Identical Values for μ

However, reducing μ for the filter with more weight results in the following comparison in Figure 5.7, where the 6 weight vector has an improved error response over the 4 weight filter.

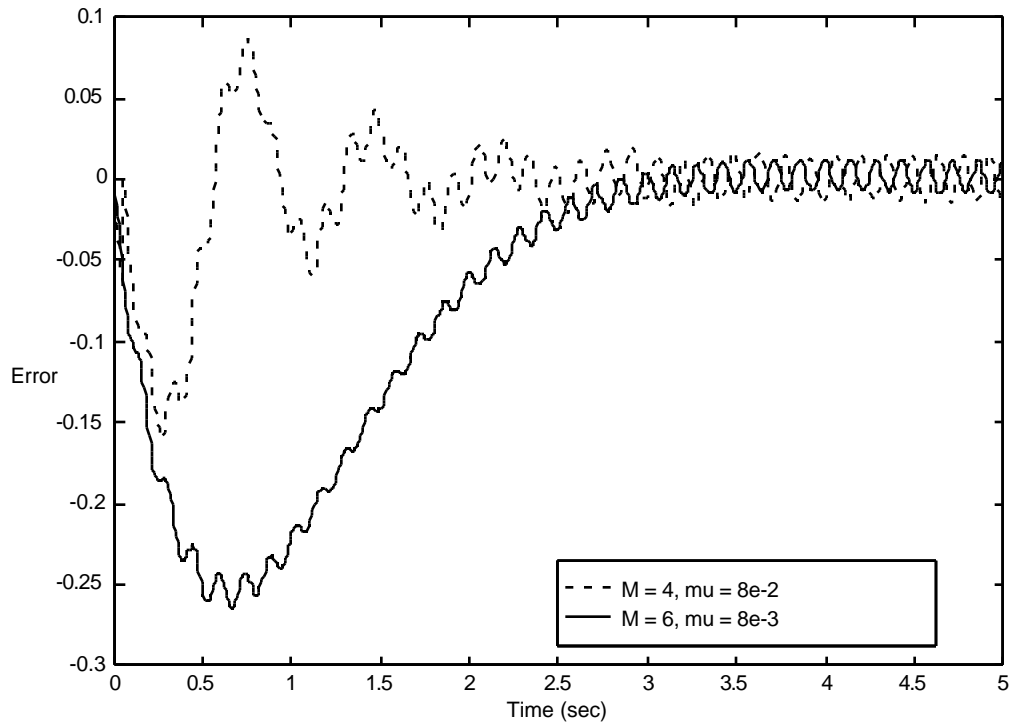


FIGURE 5.7 Comparison of Error Responses for Varying Number of Adaptive Weights and Different Values for μ

The amplitude of the error after convergence for the 6 weight filter was $1.91e-2$ whereas the amplitude was $2.87e-2$ for the 4 weight vector. Algorithm convergence time is of course increased however as more weights are added to the filter, as is evident in Figures 5.6 and 5.7.

So depending on the application and how fast convergence is required, μ and the number of weights can be optimized if needed, although the analysis can become quite cumbersome computationally.

5.1.4 Effect of the Sampling Rate

The continuous motion of any system is discretized when it is sampled, and thus the interpretation of the system is a direct result of the sampling rate. Also as a result of the sampling process is a time lag introduced into the system. Sampling data and determining the control required takes a finite amount of time and so on average the discrete-time control signal is delayed by half a sample period compared to the continuous-time control signal. This delay introduces a phase lag into the system, which will hamper the effects of the closed-loop performance. Thus the choice of sampling rate is very important [Åström, 1990]. This section will discuss the effects of the choice of the sampling rate.

Figure 5.8 shows a comparison of the error time responses for three different choices of the sampling period, T . The plot for $T = 1/200$ is shown with a bias of +0.1 and the plot for $T = 1/400$ is shown here with a bias of -0.1 for ease in reading the graph (i.e. all three cases do converge about zero).

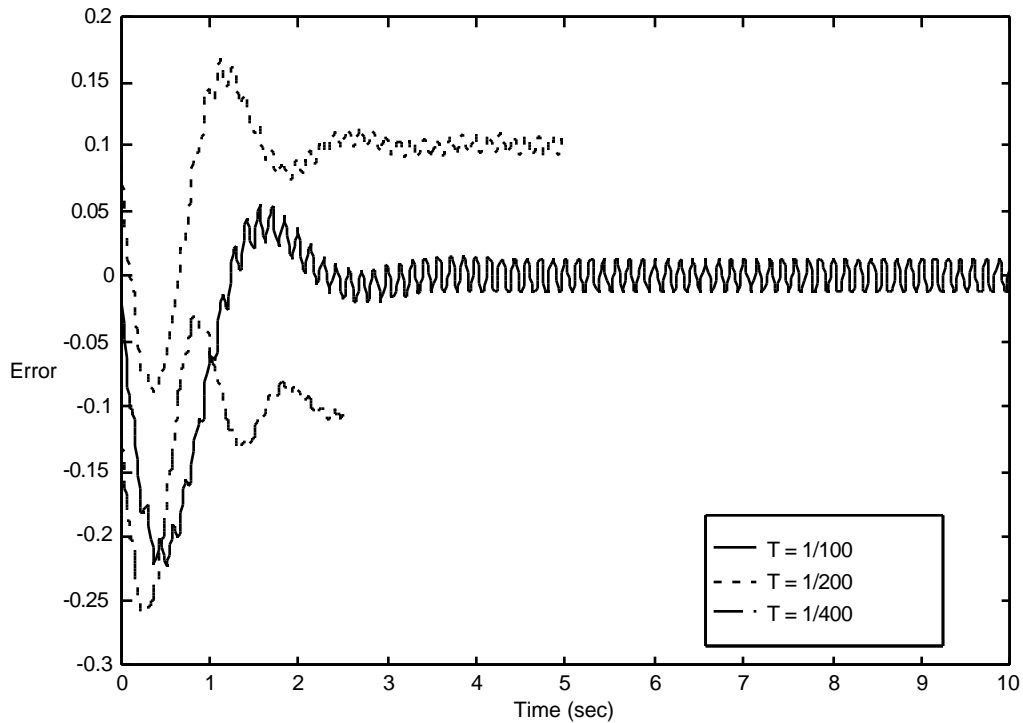


FIGURE 5.8 Comparison of Error Time Responses for Different Values of T

As can be seen, the amplitude of the oscillations varies with T. As T decreases, Figure 5.8 indicates that the amplitude of the oscillations will decrease, and the convergence time will improve as well. This makes sense intuitively, because as the sampling frequency increases, the algorithm has a more accurate representation of the system and the time interval between weight updates is smaller. Thus there is not as much over-compensation in the descent to find the minimum mean-square error. So these trends tell us that as fast a sampling rate as can be tolerated computationally should be used to improve convergence and algorithm performance.

5.1.5 Discussion of Generalized Time-Periodic System Results

The filtered-X LMS algorithm was shown to successfully converge and reduce the error from the open-loop case for a generalized first-order system. In addition, it has been shown that choice of the convergence parameter μ , the number of weights, and the sampling rate can all greatly influence the performance of the adaptive algorithm for time-periodic systems. The choice of each parameter influences the choice of the other parameters during algorithm implementation. Thus there is no set of rules to follow to produce desirable results when implementing the filtered-X LMS algorithm. Some general trends have been shown, and should guide the control design in the quest for minimal mean-square error. The following sections discuss the performance of the filtered-X LMS algorithm for the specific case of a helicopter rotor blade system.

5.2 Helicopter Rotor Blade System

The second system explored in this investigation was that of a helicopter rotor blade in forward flight. First the motivation behind using this system as an example for the application of the filtered-X LMS algorithm will be discussed. Then the system will be described, and finally the results will be shown.

5.2.1 Motivation for Application of Controller to Rotor Blade

The demand for increasing helicopter usage for passenger transportation and defense purposes has underlined the need for vibration reduction. Helicopters are plagued with vibrations caused by the rotating blades which limit their usefulness. High hub forces,

transmitted through the rotor shaft to the engine mounts, reduce passenger and pilot comfort and reduce the fatigue life of the helicopter components. Maintenance costs are also significantly increased due to the vibrations. A reduction in these vibrations would improve the economical burdens associated with helicopters and increase usage in both the military and commercial sectors. An increase in the operational life of the components and a reduction in maintenance costs would also result from such an improvement in rotorcraft [Sivaramakrishnan and Venkatesan, 1990].

Due to increasingly more stringent restrictions on permissible vibration levels, helicopter research efforts have and will continue to increase in this area. Over the past 40 years efforts to reduce helicopter vibrations have experienced great progress. Helicopter cabin vibration levels were reduced by a factor of almost 6 (from 0.6g to 0.1 g) during the period between 1955 to 1985. This is a significant reduction, however requirements for even lower levels continue to challenge the industry. For example, the NASA Research and Technology Advisory Council Subpanel on Helicopter Technology recommended a desirable level of 0.02 g in 1976. Thus, further progress is still needed. Supporting these restrictions are the well-known Goldman-data, or tolerance criteria, which show that vibration levels above around 0.1 g are uncomfortable to pilots and passengers. Pilots and passengers are not willing to accept such high vibration levels as are currently experienced. The present situation is unsatisfactory to the helicopter industry and so research efforts in this area are imperative [Reichert, 1981].

It has been established that research in the area of helicopter vibration suppression is required by the industry. The helicopter vibration problem is very complex in nature however. The following paragraphs will briefly explain the nature of these vibrations.

5.2.2 Equation of Motion

The dynamics of a helicopter blade become periodic due to the unsteady asymmetrical flow over the airfoil as it traverses the azimuth. When a helicopter is in forward flight, oscillating airloads on the rotor blades result from this non-uniform flow of air passing through the rotor. These airloads cause periodic excitation forces and moments at the rotating hub at the following frequencies:

$$(n - 1) \Omega, n \Omega, (n + 1) \Omega$$

where n is a multiple of the number of blades and Ω is the rotational frequency of the rotor. These forces and moments are transmitted from the rotating hub system to the fixed fuselage system at frequencies of $n \Omega$, where n is again a multiple of the number of blades. Thus the rotor has filtered some of the frequencies (those at $(n - 1) \Omega$ and $(n + 1) \Omega$).

The equation of motion considered here for the rotor blade was for motion in the flapping direction, β , only (perpendicular to the plane of rotation, or β). Derived by Bramwell [1976], the equation is

$$\frac{d^2\beta}{dt^2} + (a_1 + a_2 \sin(\Omega t)) \frac{d\beta}{dt} + (a_3 + a_4 \cos(\Omega t) + a_5 \sin(2\Omega t))\beta = bu + d \quad (5.2.1)$$

where the coefficients on the left side of the equation are defined as

$$a_1 = \frac{\gamma}{8} ; a_2 = \frac{\gamma \mu}{6} ; a_3 = \Omega^2 (1 + \epsilon) ; a_4 = \frac{\gamma \Omega^2 \mu}{6} ; a_5 = \frac{\gamma \Omega^2 \mu^2}{8} \quad (5.2.2)$$

The input coefficient b is defined as

$$b = \frac{\Omega^2 \gamma}{8} \quad (5.2.3)$$

The disturbance input, d , is defined as

$$d = d_1 + d_2 \sin(\omega t) + d_3 \sin^2(\omega t) + d_4 \cos(\omega t) \quad (5.2.4)$$

where

$$d_1 = \frac{\gamma^2}{8} \theta_0 + \frac{4}{3} \lambda \quad ; \quad d_2 = \frac{\gamma^2 \mu}{4} \frac{4}{3} \theta_0 + \lambda \quad ; \quad d_3 = \frac{\gamma^2 \theta_0 \mu^2}{4} \quad ; \quad d_4 = -1.46 \frac{\gamma^2 \sqrt{u} \lambda_i}{8} \quad (5.2.5)$$

This disturbance is modeled as described in equations 2.2.8 - 2.2.10 of section 2.2.1.

These equations result in

$$A_d = \begin{bmatrix} 0 & 0 & 0 & 0 & 1 & 0 \\ 0 & 0 & 1 & 0 & 0 & 0 \\ 0 & 0 & 0 & 1 & 0 & 0 \\ 0 & 0 & -4 \omega^2 & 0 & 0 & 0 \\ 0 & 0 & 0 & 0 & 0 & 1 \\ 0 & 0 & 0 & 0 & -\omega^2 & 0 \end{bmatrix} \quad (5.2.6)$$

and

$$C_d = [1 \ 1 \ 0 \ 0 \ 0 \ 0] \quad (5.2.7)$$

The variables in equations 5.2.2 through 5.2.5 were taken from common values used by Nitzsche [1994], Millott and Friedmann [1992], and Bramwell [1976] for articulated rotor blades. These values are listed in Table 5.1.

TABLE 5.1 Helicopter Rotor Blade Variables

Variable	Definition	Value
	Lock's inertia number	6.0
μ	rotor advance ratio	0.3
	hinge offset	0.06
θ_0	collective pitch angle	12°
	inflow ratio	0.0465
i_0	$i_0 / (R)$	0.0071
R	rotor radius	4.926 m
v_i	induced velocity	10.2 m/s
	rotor rotational frequency	44.5 rad/sec

These equations are for the first harmonic only and model the blade as a rigid beam with a flapping hinge. It is also assumed that the collective pitch angle is constant. The equations are only valid for the advancing region ($0^\circ < \psi < 180^\circ$, where 0° is the rear of the helicopter) since the issue of reverse flow is neglected. Bramwell [1976] states that these assumptions result in negligible error for the speeds typical of present-day helicopters.

The control input in this investigation is an actuator at the root of the blade that changes the blade pitch. The control was implemented with the desired response equal to the coning angle $\theta_0 = 6^\circ$. The coning angle is the angle at which the blade weight is supported by aerodynamic lift for a blade in hover [Seddon, 1990] (i.e. its equilibrium angle).

5.2.3 Results

Figures 5.9 through 5.2.12 show the resulting error, control input, and weight vectors as a function of time for the helicopter rotor blade system. The algorithm used to generate these results consisted of 8 adaptive weights, with a convergence parameter of $\mu = 8e-2$.

The sampling rate used was 200 Hz, or 28.2 times the rotor rotational frequency.

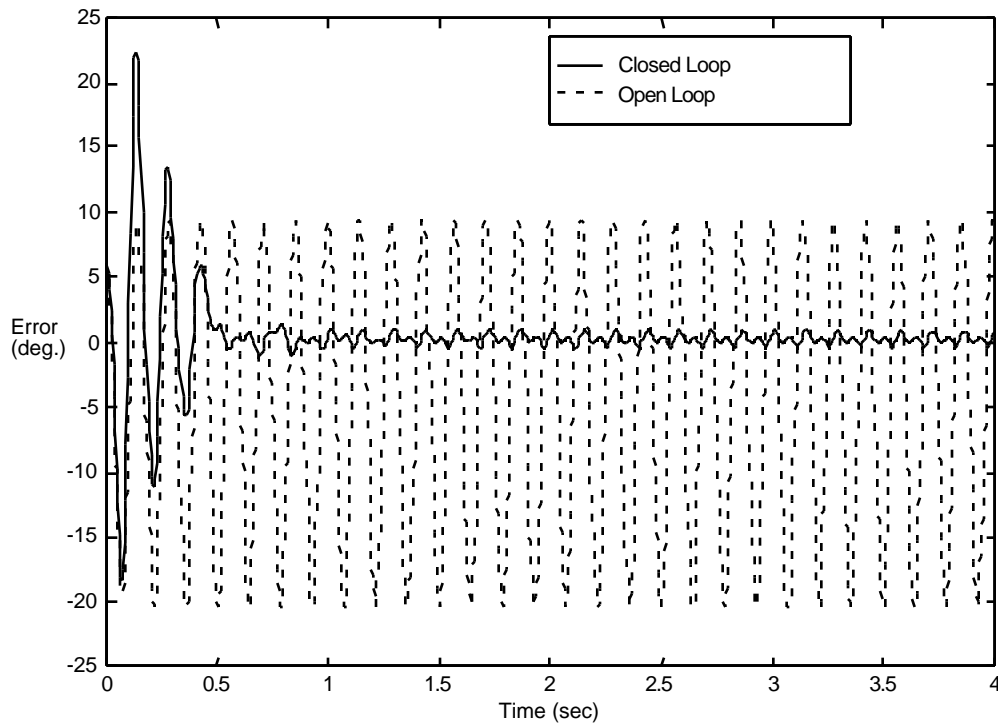


FIGURE 5.9 Error Time Response for Helicopter Rotor Blade System

Looking at Figure 5.9 we see that at steady state the closed-loop error oscillates $\pm 0.6^\circ$ with an offset, or mean value, of 0.14° . In comparison, the open-loop error oscillates $\pm 15^\circ$ with a mean value of -4.78° . Thus the filtered-X LMS controller has reduced the error by about 96%. The large reduction in closed-loop error as compared to

the open-loop system translates to a large reduction in vibration levels. This is especially true for the helicopter rotor blade system in which even small reductions have significant benefits in industry.

It is also of interest to note the shape of the error response. Looking at only the error between 3.5 and 4 seconds in Figure 5.10, we see that the response has a very complicated waveform. This is due to the periodic nature of the system and the higher order terms evident in the system dynamics (i.e. the $\sin(2t)$ and $\sin^2(t)$ terms).

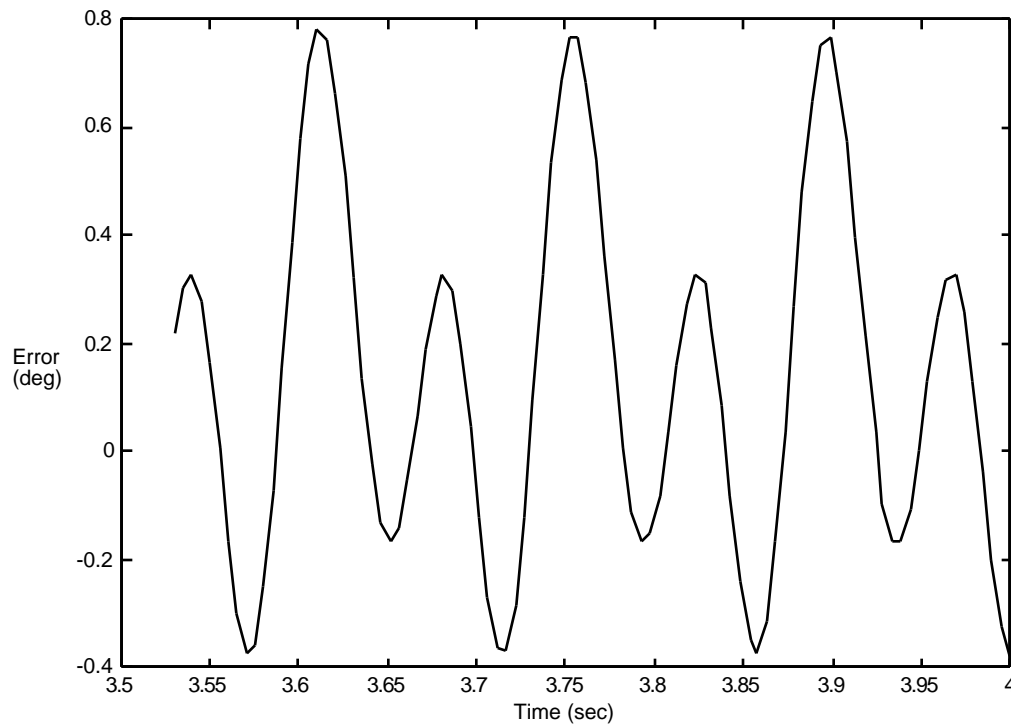


FIGURE 5.10 Close-Up of Error Time Response for Helicopter Rotor Blade System

The resulting control input is shown in Figure 5.11. Due to the time-periodicity of the system, the control input is periodic as well.

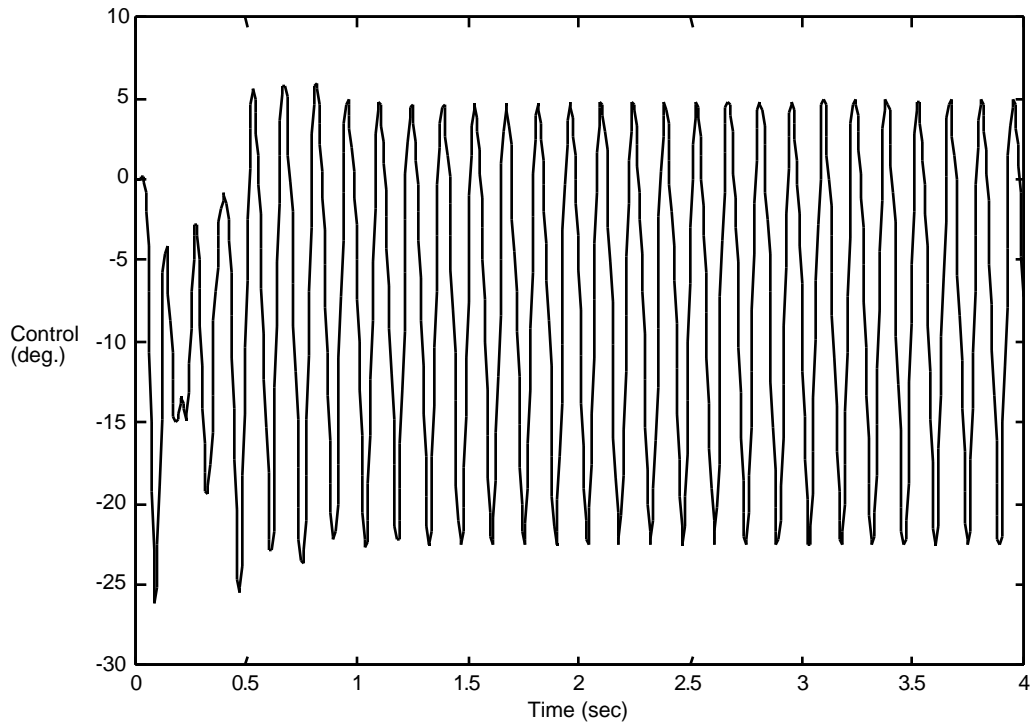


FIGURE 5.11 Control Input Time Response for Helicopter Rotor Blade System

The 8 weights required for these results are shown in Figure 5.12. A close-up of the seventh weight in Figure 5.13 demonstrates that the weights are periodic as well.

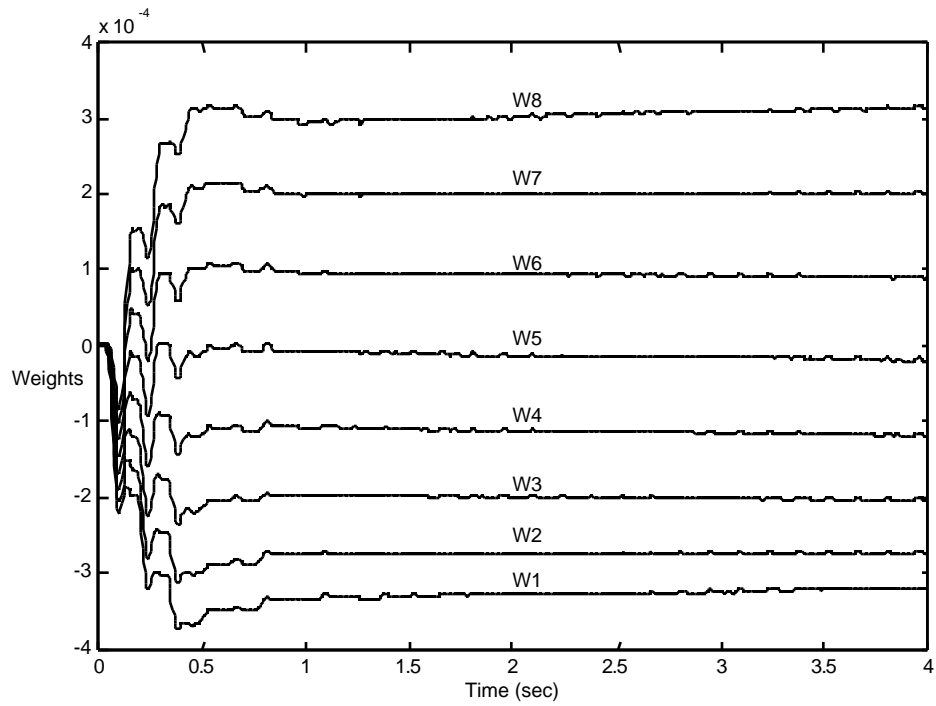


FIGURE 5.12 Weight Vector Time Responses for Helicopter Rotor Blade System

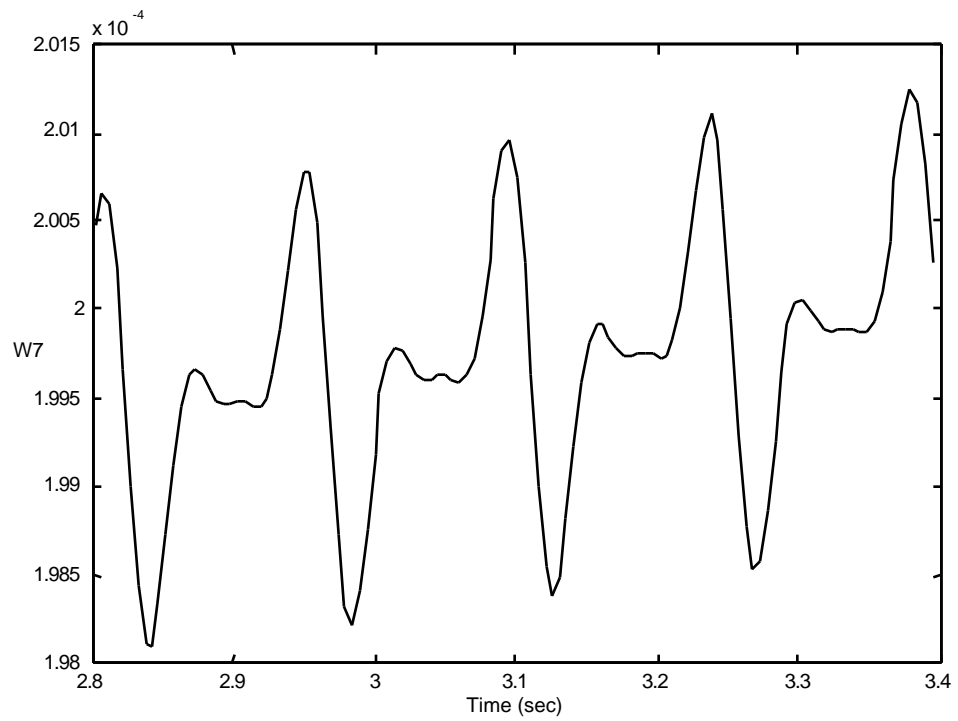


FIGURE 5.13 Close-up of Time Response of 7th Weight

Thus we see that with the filtered-X LMS algorithm we are able to develop a controller which successfully reduces vibrations in Bramwell's model of a helicopter rotor blade significantly. Comparison of the open- and closed-loop error plots shown in Figure 5.9 should warrant further investigation of this algorithm with more complex models of the helicopter rotor blade system.

Note that for both the generalized system of section 5.1 and the helicopter system the expected value of the error never reaches exactly zero. Looking at adaptive controller theory for time-invariant systems one might believe that the error should converge to zero for time-varying systems as well. The following section analytically investigates the convergence of the error for time-periodic systems.

5.3 Controller Error

The results show that the error never quite reaches zero in the filtered-X LMS algorithm for time-varying systems. Intuitively, we would expect that the error might oscillate about zero, although the amplitude of the oscillations could be small. However, we must remember that the minimum mean-square error is nonstationary for time-varying systems. Thus, it might not be possible to find this minimum. In fact, this inability of the algorithm to produce zero error for time-periodic systems can be proved analytically. This will be shown using the inverse modeling algorithm used in deriving the filtered-X LMS algorithm for a first order system.

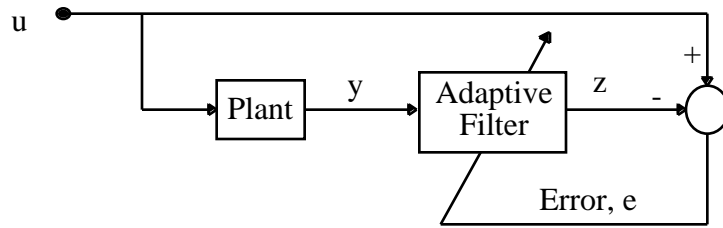


FIGURE 5.14 Inverse Plant Modeling

The discrete model of the plant is

$$y_n = a_n y_{n-1} + b_n u_n \quad (5.3.1)$$

where n is the iteration number. The equation for the adaptive filter is

$$z_n = w_{0,n} y_n + w_{1,n} y_{n-1} = w_n^T \bar{y}_n \quad (5.3.2)$$

where

$$\bar{y}_n = [y_n \ y_{n-1} \ \dots \ y_{n-p}]^T \quad (5.3.3)$$

for p filter weights. The error is defined as

$$e_n = u_n - z_n \quad (5.3.4)$$

Solving equation 5.3.1 for u_n results in

$$u_n = \frac{1}{b_n} y_n - \frac{a_n}{b_n} y_{n-1} \quad (5.3.5)$$

assuming $b_n \neq 0$ for all n . For an error equal to zero, equation 5.3.4 results in $u_n = z_n$.

Thus, from equation 5.3.5 the optimum filter weights are

$$w_{opt,n} = \begin{matrix} 1/b_n \\ -a_n/b_n \end{matrix} \quad (5.3.6)$$

This also shows that for a first order system of this type (i.e. auto-regressive form), only 2 filter weights are necessary. Similarly, it can be shown that for a second order system of this form, 3 weights are required to result in zero error. (Each time the order of the system increases, an additional weight is needed.)

If this is the optimum weight vector, let's look at how the weight vector w_n compares to $w_{opt,n}$ for all n . If $b_n = 1$ and $a_n = a_1 + a_2 \sin(2\pi n/m)$ where m is the period, at time $n+1$ the optimum weight vector will be

$$w_{opt,n+1} = \begin{matrix} 1 \\ -a_1 - a_2 \sin \frac{2\pi(n+1)}{m} \end{matrix} \quad (5.3.7)$$

This can be rewritten as

$$w_{opt,n+1} = \begin{matrix} 1 \\ -a_1 - a_2 \sin \frac{2\pi n}{m} + a_2 \sin \frac{2\pi n}{m} - a_2 \sin \frac{2\pi(n+1)}{m} \end{matrix} \quad (5.3.8)$$

or

$$w_{opt,n+1} = \begin{matrix} 1 \\ -a_1 - a_2 \sin \frac{2\pi n}{m} \end{matrix} + \begin{matrix} 0 \\ -a_2 \sin \frac{2\pi(n+1)}{m} - \sin \frac{2\pi n}{m} \end{matrix} \quad (5.3.9)$$

which simplifies to

$$w_{opt,n+1} = w_{opt,n} - f_n \quad (5.3.10)$$

where f_n is termed a forcing function. To examine the error e_n between the optimal weight vector and the weight vector at any time n , we define again the LMS algorithm as

$$w_{n+1} = w_n + \mu \bar{y}_n e_n \quad (5.3.11)$$

where μ is the convergence parameter. Thus at time $n+1$ this error becomes

$$\varepsilon_{n+1} = w_{n+1} - w_{opt,n+1} = w_n + \mu \bar{y}_n e_n - w_{opt,n} + f_n \quad (5.3.12)$$

Rearranging terms and simplifying reduces equation 5.3.12 to

$$\varepsilon_{n+1} = (I - \mu \bar{y}_n \bar{y}_n^T) \varepsilon_n + f_n \quad (5.3.13)$$

Thus the error will never be exactly zero due to the forcing function term f_n . The weights will always lag the optimal weight vector $w_{opt,n}$. This equation defining f_n also suggests that as $m \rightarrow \infty$, the sine terms will approach zero, thus causing $f_n \rightarrow 0$. This implies that slower plants may be easier to track.

Chapter 6

Conclusions

Disturbance rejection for time-periodic systems using the filtered-X LMS algorithm has been presented. In this work the discrete form of the solution to the differential equation for time-periodic continuous systems was derived. Considerations for time-varying systems were also discussed for the filtered-X LMS algorithm. Specifically, it was determined that the Wiener solution used to find the optimal weights in the filtered-X LMS algorithm is invalid for time-periodic systems. This is due to the fact that x_k is statistically nonstationary signals and the weight vector \mathbf{W} is not constant—properties which invalidate the assumptions used in the derivation of the Wiener solution. During adaptation, the error is nonstationary as the weight vector attempts to converge to the optimal weight vector. The adaptive process tracks a performance curve to find the minimum MSE at the “bottom of the bowl”. However, for nonstationary systems the bottom of the bowl is moving in time, thus complicating the convergence process. This results in excess mean-square error, such that the error can never be exactly zero as it can for time-invariant systems.

In addition to this complication, the time-varying system creates additional constraints on the algorithm. It was found that the best performance of the filtered-X LMS algorithm must be found by a compromise between fast adaptation which is needed to track variations in the input statistics, and slow adaptation which is necessary to minimize the noise entering the LMS algorithm [Widrow, *et al.*, 1976]. Thus a plot of the some cost function versus the convergence parameter can be performed in order to optimize convergence time and minimize the error.

The implementation of the filtered-X LMS algorithm was shown for two systems. For the first system, a first-order generalized system, application of the algorithm was shown to converge and reduce the error (to oscillate about zero) from the open-loop case. In addition, the influence of the convergence parameter μ , the number of filter weights, and the sampling rate were all shown to have significant impact on the performance of the algorithm. Specifically, it was shown that these variables directly influence one another, although not in a cookbook way. In other words, there are not a set of strict rules used in the design of a filtered-X LMS controller for time-periodic systems to produce the minimum mean-square error. General trends were discussed but choice of these parameters must be experimented with for each system individually.

The second system examined in this work was that of a second-order model of a helicopter rotor blade derived by Bramwell [1976]. This model was for the flapping motion of the blade only. Ninety-six percent, or 14 dB, reductions in the error were obtained from the open-loop case. This results in significant reductions in the vibrations of the blade in the flapping direction. The trends discussed for the generalized system were verified with this system as well. With the adaptive nature of this algorithm, robustness to modeling errors may be good, especially when compared to the higher harmonic controllers currently used in industry. These promising results warrant further investigation of the performance of the filtered-X LMS algorithm for more complex models of the helicopter rotor blade system.

References

Ackermann, Jürgen. *Sampled-Data Systems*. New York: Springer-Verlag, 1985.

Aeyels, D., and J. Willems. "Pole Assignment for Linear Time-Invariant Second-Order Systems by Static Output Feedback," *IMA J. Math. Contr. Inform.*, 1991, Vol. 8, pp 267-274.

Aeyels, D., and J. Willems. "Pole Assignment for Linear Time-Invariant Systems by Periodic Memoryless Output Feedback," *Automatica*, 1992, Vol. 28, pp 1159-1168.

Aeyels, D., and J. Willems. "Pole Assignment for Linear Periodic Systems by Memoryless Output Feedback," *IEEE Transactions on Automatic Control*, April 1995, Vol. 40, No. 4, pp 735-739.

Åström, K., and B. Wittenmark. *Computer-Controlled Systems, 2nd. ed.* Englewood Cliffs, New Jersey: Prentice Hall, 1990.

Bramwell, A. *Helicopter Dynamics*. London, U.K.: Edward Arnold Ltd., 1976.

Calico, R., and W. Wiesel. "Control of Time-Periodic Systems," *Journal of Guidance, Control, and Dynamics*, Nov.-Dec. 1984, Vol. 7, No. 6, pp 671-676.

Calise, A., Wasikowski, M., and D. Schrage. "Optimal Output Feedback for Linear Time-Periodic Systems," *Journal of Guidance, Control and Dynamics*, Mar.-Apr. 1992, Vol. 15, No. 2, pp 416-423.

Chen, C. *Linear System Theory and Design*. New York: Holt, Rinehart and Winston, Inc., 1984.

Cunningham, W. *Introduction to Nonlinear Analysis*. New York: McGraw-Hill Book Company, Inc., 1958.

Fowler, L., Cole, D., Robertshaw, H., and V. Guirguitiu. "Individual Feedforward-Feedback Control of a Flexible Rotor Blade — A Comparison of Approaches," *1995 North American Conference on Smart Structures and Materials*, February 1995, pp 423-431.

Franklin, G., Powell, J., and M. Workman. *Digital Control of Dynamic Systems, 2nd ed.* New York: Addison-Wesley Publishing Company, 1990.

Giurgiutiu, V., Z. Chaudhry and C. Rogers. "Active Control of Helicopter Rotor Blades with Induced Strain Actuators," AIAA paper No. 94-1765, *Proceedings of the 35rd AIAA/ASME/ASCE/AHS/ASC Structures, Structural Dynamics, and Materials Conference and Adaptive Structures Forum*, April 1994, pp 1-10.

- Grasselli, O, and S. Longhi. "Disturbance Localization by Measurement Feedback for Linear Periodic Discrete-time Systems," *Automatica*, 1988, Vol. 24, No. 3, pp 375-385.
- Hale, F. *Introduction to Control System Analysis and Design, 2nd ed.* Englewood Cliffs, New Jersey: Prentice Hall, 1988.
- Hall, S., and N. Werely. "Linear Control Issues in the Higher Harmonic Control of Helicopter Vibrations," *Proceedings of the 45th Annual Forum of the American Helicopter Society*, 1989, pp 955-971.
- Ham, N. "Helicopter Individual-Blade-Control and Its Applitcations," *Proceedings of the 39th Annual National Forum of the American Helicopter Society*, St. Louis, Mo., May 1983.
- Jacklin, S., J. Leyland and A. Blaas. "Full-Scale Wind Tunnel Investigation of a Helicopter Individual Blade Control System," AIAA paper No. 93-1361-CP, *Proceedings of the 34th AIAA/ASME/ASCE/AHS/ASC Structures, Structural Dynamics, and Materials Conference*, California, pp 576-586, April 1993.
- Johnson, W. "Self-tuning Regulators for Multicyclic Control of Helicopter Vibration," *NASA Technical Paper 1996*, 1982.
- Knospe, C., and J. Haviland. "Pulse Response Method for Vibration Reduction in Periodic Dynamic Systems," *Journal of Guidance, Control, and Dynamics*, 1991, Vol. 15, No. 3, pp 782-785.
- Millott, T. and P. Friedmann . "Vibration Reduction in Helicopter Rotors Using an Active Control Surface Located on the Blade," AIAA paper No. 92-2451, *Proceedings of the 33rd AIAA/ASME/AHS/ASC Structures, Structural Dynamics, and Materials Conference*, pp 1975-1988, April 1992.
- Nitzsche, F. and E. Breitbach. "A Study of the Feasibility of Using Adaptive Structures in the Attenuation of Vibration Characteristics of Rotary Wings," AIAA paper No. 92-2452, *Proceedings of the 33rd AIAA/ASME/AHS/ASC Structures, Structural Dynamics, and Materials Conference*, Part 3, pp 1391-1402, April 1992.
- Nitzsche, F. "Designing Efficient Helicopter Individual Blade Controllers Using Smart Structures," AIAA paper No. 94-17662451, *Proceedings of the 35rd AIAA/ASME/AHS/ASC Structures, Structural Dynamics, and Materials Conference*, pp 298-308, April 1994.
- Ogata, K. *Modern Control Engineering*. Englewood Cliffs, New Jersey: Prentice Hall, 1990.
- Reader, K., and W. Dixon, Jr. "Evaluation of a Ten-Foot Diameter X-Wing Rotor," *Proceedings of the 40th Annual National Forum of the American Helicopter Society*, Arlington, Va., May 1984.
- Reichert, G. "Helicopter Vibration Control — A Survey," *Vertica*, Vol. 5, pp 1-20, 1981.

Robinson, L. and P. Friedmann. "A Study of Fundamental Issues in Higher Harmonic Control Using Aeroelastic Simulation," *Journal of the American Helicopter Society*, Vol. 36, No. 2, April 1991, pp 32-43.

Seddon, J. *Basic Helicopter Aerodynamics*. London, U.K.: Blackwell Scientific Publications, 1990.

Shaw, J. and N. Albion. "Active Control of the Helicopter Rotor for Vibration Reduction," *Proceedings of the 36th Annual Forum of the American Helicopter Society*, Washington, D.C., May 1980.

Shaw, J., Albion, N., Hanker, E. J. and R. S. Teal. "Higher Harmonic Control: Wind Tunnel Demonstration of Fully Effective Vibratory Hub Force Suppression," *Journal of the American Helicopter Society*, Vol. 34, No. 1, Jan. 1989, pp. 14-25.

Sievers, L., and A. von Flotow. "Comparison and Extensions of Control Methods for Narrow-Band Disturbance Rejection," *IEEE Transactions on Signal Processing*, Oct. 1992, Vol. 40, No. 10, pp 2377-2391.

Sinha, S., Wu, D., Juneja, V., and P. Joseph. "Analysis of Dynamic Systems With Periodically Varying Parameters Via Chebyshev Polynomials," *Journal of Vibration and Acoustics*, Jan. 1993, Vol. 115, pp 96-102.

Sivaramakrishnan, R. and C. Venkatesan. "Rotor/Fuselage Vibration Isolation Studies by a Floquet-Harmonic Iteration Technique," *Journal of Aircraft*, Vol. 27, No. 1, pp 81-89, Jan. 1990.

Sreedhar, J., and P. Van Dooren. "Pole Placement Via the Periodic Schur Decomposition," *Proceedings of the 1993 American Control Conference*, June 1993, pp 1563-1567.

Sreedhar, J., and P. Van Dooren. "On Finding Stabilizing State Feedback Gains for a Discrete Time-Periodic System," *Proceedings of the 1994 American Control Conference*, June 1994, Vol. 1, pp 1167-1168.

Walgama, K. and J. Sternby. "A Feedforward Controller Design for Periodic Signals in Non-Minimum Phase Processes," *International Journal of Control*, 1995, Vol. 61, No. 3, pp 695-718.

Widrow, B., McCool, J., Larimore, M., and C. Johnson, Jr. "Stationary and Nonstationary Learning Characteristics of the LMS Adaptive Filter," *Proceedings of the IEEE*, Aug. 1976, Vol. 64, No. 8, pp 1151-1162.

Widrow, B., and S. D. Stearns. *Adaptive Signal Processing*. Englewood Cliffs, New Jersey: Prentice Hall, 1985.

Widrow, B., and E. Walach. "On the Statistical Efficiency of the LMS Algorithm with Nonstationary Inputs," *IEEE Transactions on Information Theory*, March 1984, Vol. IT-30, No. 2, pp 211-221.

Wolovich, W. *Automatic Control Systems*. New York: Saunders College Publishing, 1994.

Vita

Leslie Fowler was born January 31, 1972 in Newport News, Virginia. She grew up in Yorktown, Virginia and graduated from York High School. Miss Fowler obtained her Bachelor of Science from Virginia Polytechnic Institute and State University in Mechanical Engineering in 1994. She also obtained a minor in Music — Vocal Performance, and had the privilege of singing the national anthem and Virginia Tech's alma mater at graduation. In addition, she participated in several operas at Opera Roanoke and performed in two solo vocal recitals. As an undergraduate she worked at Canon Virginia, Inc. in Newport News, Virginia as a Mechanical Product Engineering Co-Op for four summers. In 1994 she was the ARO/CIMSS (Army Research Office/Center for Intelligent Material Systems and Structures) Summer Research Intern where she completed an initial investigation of the helicopter rotor blade vibration problem. Intrigued by the field of controls, she continued her education in graduate school at Virginia Tech. After receiving her Master of Science in Mechanical Engineering in May 1996, she will move to Erie, PA with her husband-to-be (May 25, 1996), Christian Fowler (sic), where she will work as a Mechanical Engineer at Lord Corporation. Leslie plans to continue her professional singing in her free time.

Leslie P. Fowler